Article (refereed) - postprint

Valach, A.C.; Langford, B.; Nemitz, E.; MacKenzie, A.R.; Hewitt, C.N. 2014.
Concentrations of selected volatile organic compounds at kerbside and background sites in central London.

Contact CEH NORA team at
noraceh@ceh.ac.uk

1 # Concentrations of selected volatile organic compounds at
2 # kerbside and background sites in central London

3

4 **A. C. Valach[a], B. Langford[b], E. Nemitz[b], A. R. MacKenzie[c] and C. N. Hewitt[a]**

5 [a]{Lancaster Environment Centre, Lancaster University, Lancaster, LA1 4YQ, United Kingdom

6 (a.valach@lancaster.ac.uk; n.hewitt@lancaster.ac.uk)}

7 [b]{Centre for Ecology & Hydrology, Bush Estate, Penicuik, Midlothian, EH26 0QB, United Kingdom

8 (benngf@ceh.ac.uk; en@ceh.ac.uk)}

9 [c]{School of Geography, Earth and Environmental Sciences, University of Birmingham, Edgbaston,

10 Birmingham, B15 2TT, United Kingdom (a.r.mackenzie@bham.ac.uk)}

11 Correspondence to: A.C. Valach (a.valach@lancaster.ac.uk

12

15 **Abstract**
16 Ground-level concentrations of nine volatile organic compounds (VOCs) were measured using a
17 proton transfer reaction-mass spectrometer (PTR-MS) in central London at an urban background
18 (North Kensington, NK, during 16th - 25th Jan 2012) and a kerbside site (Marylebone Rd, MRd, during
19 25th Jan - 7th Feb 2012) as part of the winter intensive observation period of the ClearfLo project. Site
20 comparisons indicated that VOC concentrations at the urban background site were significantly
21 lower than at the kerbside site (ratio MRd/NK of 2.3). At the kerbside site PTR-MS measurements of
22 aromatics (benzene, toluene, C_2- and C_3-benzenes) were compared with the gas chromatography –
23 flame ionization detector data from the UK Government's Automatic Hydrocarbon Network. Very
24 good qualitative agreement was observed between the two methods (r = 0.90 - 0.91, p<0.001, N =
25 260), although there was a significant offset between the instruments. This was partly due to issues
26 with humidity dependent background measurements, but possibly also from isobaric interference of
27 other compounds and their fragments, giving a positive bias to the PTR-MS data. Most compounds
28 showed strong indications of traffic-related sources with double rush hour peaks in diurnal profiles
29 and high correlations with known traffic-related compounds (r = 0.68 - 0.97 at NK , 0. 48 - 0.87 at
30 MRd, p <0.001, N_{NK} = 2202-2227, N_{MRd} = 2705-2720) and CO (r = 0.80-0.96 at NK, 0.65-0.84 at MRd, p

31 <0.001, N_{NK} = 223, N_{MRd} = 256-274). Polar plots agreed with statistical analysis of wind direction

32 dependency and identification of potential emission sources was attempted.

1 Introduction

34 Anthropogenic sources of volatile organic compounds (VOCs) are of particular importance in urban

35 areas due to the intensity of fossil fuel combustion and the relative paucity of biogenic sources in

36 cities. A wide range of VOCs are emitted directly by the evaporation of fuels and solvents, as unburnt

37 fuel and as partially oxidized compounds from combustion processes, mostly vehicle emissions

38 (Kansal, 2009). Some VOCs can directly affect human health (e.g. benzene, which is a known

39 carcinogen) while others contribute to the formation of ozone and aerosol particles in the

40 atmosphere (Derwent, 1995). Both have detrimental effects on human health and the environment

41 (Kim et al., 2001). In winter elevated VOC concentrations are observed due to the shallow daytime

42 boundary layer with limited dilution and mixing. In the UK, VOC emissions are subject to control

43 under European Commission Directive 2008/50/EC. Monitoring networks such as the Automatic

44 Hydrocarbon Network (AHN) provide a running annual mean concentration for a suite of pollutants.

45 Emissions are estimated as part of the National Atmospheric Emission Inventory (NAEI) activity

46 (Yardley et al., 2012).

47 A wide range of studies focus on VOC concentrations and air quality in cities around the world using

48 diverse measuring techniques (Baker et al., 2008; Jobson et al., 2010). Due to the variety of emission

49 sources, meteorological conditions, and often short atmospheric lifetimes of the compounds, VOC

50 volume mixing ratios can be associated with large variability. Slow response instruments have

51 identified seasonal and diurnal patterns of urban VOC concentrations (Kim et al., 2001), however

52 only fast response instruments have been shown to record this short term variability.

53 The aim of this study was to:

54 I. Quantify a suite of VOCs at an urban background and a kerbside site in winter and;

55 II. Compare VOC volume mixing ratios from fast response PTR-MS measurements with the GC-

56 FID measurements from the Automatic Hydrocarbon Network.

57 This study was part of the winter intensive observation period of the Clean Air for London project

58 (ClearfLo, www.clearflo.ac.uk), aimed to research boundary layer pollution over London in 2011-

59 2012 (Bohnenstengel et al., in review). Here we report measurements of nine VOC species measured

60 at high temporal resolution at a kerbside and a background site in central London (16th January - 7th

61 February 2012).

62 **2 Methods**

63 **2.1 Measurement sites and meteorology**

64 Details of both the North Kensington (NK) background and Marylebone Rd (MRd) kerbside sites are

65 compared (Supplementary content Table A1). Air was pumped through a PTFE inlet (and PTFE filter

66 at MRd) attached to 1/4" OD PTFE tubing to a high sensitivity proton transfer reaction-mass

67 spectrometer (PTR-MS; Ionicon Analytik GmbH, Innsbruck, Austria).

68 Meteorological measurements were co-located with the inlet at NK (Figure 1 and Supplementary

69 content Table A1). The mean UK temperature in January was 6.0 °C, i.e. 1.3 °C above the 1971-2000

70 average (UK Met Office, 2012), although February experienced low temperatures and snowfall,

71 which is uncommon in London.

72 **2.2 VOC sampling**

73 VOC mixing ratios were measured on-line using a PTR-MS (de Gouw and Warneke, 2007; Lindinger

74 et al., 1998). The instrument was operated in multiple ion detection (MID) and mass scan (SCAN)

75 modes (Supplementary content A1). In MID mode the quadrupole mass spectrometer scanned

76 through 11 pre-determined masses, to which the following compounds were ascribed: m/z 21

77 (indirect quantification of m/z 19 primary ion count $[H_3O^+]$ via isotopologue $[H_3^{18}O^+]$), m/z 33

78 (methanol), m/z 39 (indirectly quantified m/z 37 first cluster $[H_3O^+.H_2O^+]$), m/z 42 (acetonitrile), m/z

79 45 (acetaldehyde) m/z 59 (acetone/propanal), m/z 69 (cycloalkanes/isoprene), m/z 79 (benzene),

80 m/z 93 (toluene), m/z 107 (C_2-benzenes) and m/z 121 (C_3-benzenes).

81 The UK national Automatic Hydrocarbon Network (AHN) station at MRd measures 29 different

82 hydrocarbons using a gas chromatography-flame ionization detector (GC-FID, AutoSystem XL;

83 PerkinElmer Inc., USA). This method complies with standards set out by the European Air Quality

84 Directive (Broadway and Tipler, 2008). A 40 min continuous sampling period provides hourly means

85 (Supplementary content A2).

86 PTR-MS measures in unit mass resolution and a fragment may derive from several parent

87 compounds, therefore each detected mass may relate to one or more compounds. Where possible,

88 measurements should be verified by more specific analytical techniques, such as GC-FID.

89 Unfortunately, only benzene, toluene, some C_2- and C_3-benzenes were verified by the AHN.

90 **2.3 Quality analyses and data handling**

91 The PTR-MS was calibrated over a range of concentrations using a certified multi-component VOC

92 gas standard (Ionimed Analytik GmbH, Austria). The measured instrument sensitivities were then

93 used to convert normalized count rates of RH^+ to volume mixing ratios (Langford et al., 2010a). The

94 instrument background was quantified using a platinum catalyst and subtracted from the ambient

95 measurements. Since the background was determined for dry air, corrections for humidity effects on

96 some compounds had to be applied and were associated with large uncertainties (Supplementary

97 content B).

98 A low pass filter was applied to smooth the data and reduce instrumental noise. Spearman's rank

99 correlation coefficients and Wilcoxon rank sum tests were used in statistical analyses due to the data

100 distributions.

3 Results & Discussion

3.1 VOC concentrations

103 VOC concentrations measured by the PTR-MS at the North Kensington (NK) background site (Figure

104 2a) and at the Marylebone Rd (MRd) kerbside site (Figure 2b) are summarized in Table 1a and 1b. At

105 both sites methanol, acetaldehyde and acetone, all oxygenated compounds, were the most

106 abundant. Methanol has a variety of biogenic, anthropogenic and atmospheric sources (Cady-Pereira

107 et al., 2012). Acetone has some biogenic contributions but solvents and tailpipe emissions were

108 most likely the main sources (de Gouw et al., 2005; Reissell et al., 1999; Warneke et al., 1999). Both

109 have a low photochemical reactivity with OH resulting in longer atmospheric lifetimes, which also

110 contributed to the relatively high mixing ratios. The compounds with the lowest mixing ratios at both

111 sites were acetonitrile and cycloalkanes/isoprene. Although these are emitted from vehicle exhaust,

112 their volume mixing ratios were much lower than other traffic-related compounds. The isoprene

113 component of m/z 69 was estimated at 22% and presumably from traffic as the biogenic component

114 was absent due to the season (Borbon et al., 2001). Comparison with GC-FID isoprene

115 concentrations at NK inferred that cycloalkanes provided a significant contribution to m/z 69

116 (Supplementary content C) (Erickson et al., 2014 ;Yuan et al, 2014). Although globally biomass

117 burning is the main source of acetonitrile (Holzinger et al., 2001), in urban areas emissions from

118 vehicle exhaust are prominent as diurnal profiles resembled a double rush hour pattern (Section 3.4)

119 with some increased acetonitrile emissions occurring at low temperatures possibly from solid fuel

120 burning (Section 3.3).

121 Mixing ratios for most of the compounds agreed with or were lower than observations from other

122 urban areas, but benzene and C_2-benzenes concentrations were slightly higher at MRd compared

123 with previous observations in UK cities (Langford et al., 2009, 2010b). The measurement proximity to

124 the source emissions must be considered; for example, Langford et al. (2010b) reported

125 concentration measurements from tall towers where the effects of dilution and photochemical loss

126 are greater.

127 During both measurement periods the beginnings and ends were marked by high pollution episodes

128 (16th -18th, 24th -28th Jan and 3rd -7th Feb).

129 **3.1.1 Site comparison**

130 The volume mixing ratios of all compounds were significantly different (p <0.001) between NK and

131 MRd, except for acetone (p = 0.26). Acetone has a relatively long atmospheric lifetime (Table 1a) and

132 therefore mixing ratios are often homogenous over larger areas. Apart from methanol, which was

133 1.5 times higher at NK, the remaining compounds were up to 3 times higher at the MRd site with a

134 mean site ratio (MRd/NK) of 2.3. This difference is related to the proximity to sources and

135 differences of source strengths. Comparison of both time periods using the AHN data from MRd

136 showed that aromatic compounds were significantly higher (p<0.001) during the first period

137 indicating that the differences between the sites were indeed due to the location. These compounds

138 are found in tailpipe emissions, which so close to a heavily trafficked road was the main source. In

139 general, NK represents an urban location away from major sources and broadly representative of

140 city-wide background concentrations, e.g. urban residential areas, whereas MRd, an urban kerbside

141 site next to a major arterial route, represents central urban areas such as surrounding the

142 congestion charge zone in London.

143 **3.2 Comparisons with the Automatic Hydrocarbon Network and PTR-MS quantification**

144 **limitations**

145 Benzene, toluene, C_2- and C_3-benzenes from PTR-MS measurements were compared with the same

146 compounds or sum of compounds with similar masses measured by GC-FID in the framework of the

147 Automatic Hydrocarbon Network (AHN). Due to isobaric interference within the PTR-MS

148 measurements the sum of available GC-FID measurements was used for compounds with a

149 protonated mass of *m/z* 107 and *m/z* 121. Direct comparisons of 1h mean (±2.9-5.9% SE) PTR-MS

150 and GC-FID measurements (Figure 3) are summarized in Table 2. The PTR-MS data for these

151 compounds corresponded to within a factor of 1.3 for *m/z* 79, 93 and 107, and a factor of 2.5 for *m/z*

152 121 (p<0.001). Comparison of the time series showed that the PTR-MS measurements closely

153 followed the diurnal variations of the GC-FID measurements (Figure 3).

154 As the PTR-MS cannot distinguish between compounds with similar masses, isobaric interference

155 can occur, e.g. benzaldehyde can produce mass interferences for C_2-benzenes (Warneke et al.,

156 2003). The *m/z* 107 likely has four contributing species: ethyl benzene, (m+p)-xylene, o-xylene, and

157 some benzaldehyde. C_3- benzenes may include a wider range of compounds: propyl benzene, two

158 ethyl methyl benzenes and three trimethylbenzene isomers. The AHN measurements included all of

159 the above for m/z 107, but only three trimethylbenzene isomers at *m/z* 121.

160 Humidity dependencies on instrument sensitivities and background were thoroughly investigated in

161 the laboratory after the campaign. Calibrations showed no significant variations of sensitivity with

162 humidity. Corrections were applied to compounds showing humidity effects on instrument

163 background, but not all effects could be recreated and accounted for, such as humidity effects on

164 inlet impurities affecting aromatics (Supplementary content B).

165 Fragmentation can become a concern at higher E/N ratios (de Gouw and Warneke, 2007; Maleknia

166 et al., 2007; Warneke et al., 2003). An E/N ratio of 125 Td was used in this study as this represents a

167 compromise between reagent ion clustering and fragmentation suppression (Hewitt et al., 2003).

168 Some fragmentation can still occur, as several studies using a coupled GC-PTR-MS with a range of

169 E/N ratios have identified various fragment ions. Benzaldehyde, ethyl benzene and xylene isomers

170 with m/z 107 may produce fragments of about 30-40% at m/z 79 with higher E/N ratios (Maleknia et

171 al., 2007), as well as propyl benzene isomers and smaller contributions of fragments of butyl

172 benzene (Warneke et al., 2003). As only o-xylene was present in the calibration standard, fragments

173 from other compounds at that mass cannot be accounted for and are likely to have contributed to

174 the increased PTR-MS signal. It is estimated that with an electrical field strength of 125 Td around

175 15% C_2-benzenes may have contributed to m/z 79. Interference from fragments at m/z 93 could

176 include a range of biogenic terpenes and their isomers (Maleknia et al., 2007).

177 Previous studies have shown that there is good correlation between PTR-MS and GC-FID, however

178 the quantitative agreement can be poor with differences of up to a factor of 2 (de Gouw and

179 Warneke, 2007; Kato et al., 2004). The value for m/z 121 is somewhat higher than cited in the

180 literature, which may be due to humidity effects on inlet impurities which could not be accounted

181 for after the campaign, as well as isobaric interference from compounds and fragments not

182 measured by the AHN. All four m/z showed very good correlations (Figure 4) with r 0.90-0.91

183 (p<0.001) in agreement with literature values (Kuster et al., 2004; Langford et al., 2010b).

3.2.1 Correlations with carbon monoxide

185 Carbon monoxide (CO) concentrations were used for correlations and ratios with VOCs to determine

186 whether the VOC sources were from fuel combustion (Table 3), as CO is a suitable marker for

187 anthropogenic combustion emissions.

188 High correlations for acetonitrile against CO indicate that fuel burning was likely the primary source

189 at NK. Correlations with CO were higher for PTR-MS than GC-FID (r 0.65 – 0.75, p<0.001 for PTR-MS;

190 r 0.58-0.68, p<0.001 for GC-FID). Possibly the higher temporal resolutions and the longer sampling

191 time of the PTR-MS allowed the detection of short-term variations in emission patterns.

3.3 VOC correlations and ratios

Correlations between the different VOCs yielded coefficients (r) ranging between -0.23 and 0.97 at NK and -0.20 to 0.87 at MRd (p<0.001). The poorer correlations involved methanol (r -0.23 - 0.35). Methanol has a variety of different sources, which in this case had little commonality with the other compounds. Strong linear correlations (r 0.67 - 0.97 at NK, 0.48 - 0.87 at MRd) indicate that the other compounds shared some or almost all sources, however, bimodal distributions can relate to multiple separate sources. In winter, vehicle exhaust and, to a small extent, evaporative emissions account for a majority of the sources. The r-values at MRd were lower than at NK showing more scatter (Figure 5). This may reflect a sequential sampling artefact due to the instrument continuously cycling through the different m/z, combined with highly variable concentrations at this site. Alternatively, it may represent true variability in the nearby emission source; within traffic emissions, diverse types of vehicles, fuels, and driving patterns result in different traffic related VOC ratios (Figure 5, A and B), which can be detected by online methods as the compounds reach the inlet with little mixing (Chan et al., 1991; Chan et al., 2002).

Biomass burning for heating may explain a secondary source contribution to acetonitrile at MRd, as it mostly occurs with cold temperatures and is not shared with benzene, hence is not related to traffic emissions (Figure 5 D).

Using temperature as a third variable can illustrate temperature dependencies of source contributions. Cycloalkanes/isoprene and benzene show a good correlation (r = 0.77 and 0.80) as they are present in tailpipe emissions (Park et al., 2011) with a seasonally low biogenic component (Figure 5, E and F). The main source of most C_2- and C_3-benzenes are motor vehicle emissions (Heeb et al., 2000) which was reflected in the high correlations (0.72 to 0.97, p<0.001). These aromatics have a shorter atmospheric lifetime making them important factors in urban photochemical smog production (Table 1a).

Benzene-to-toluene (b/t) ratios can indicate the photochemical age of the pollution carried by air masses (Warneke et al., 2001 and references therein). Due to seasonally low OH concentrations, only changes in b/t ratios over longer periods were considered to be representative of air mass transport.

The median (IQR) b/t ratios were around 0.6 (0.43-0.80) at both sites and agreed with previous values (Chan et al., 2002; Heeb et al., 2000; Langford et al., 2009), as well as with those from the AHN at MRd with a median of 0.6 (0.48-0.76) (r=0.90, p<0.001). These b/t ratios are consistent with the air mass footprints derived from the UK Met Office's Numerical Atmospheric-dispersion Modelling Environment (NAME) (Jones et al., 2007) using Unified Model (UM) Met data (Figure 6).

225   This model simulates the origin of the air masses affecting the ClearfLo sites within the previous 24h

226   (Bohnenstengel et al., in review). Shifts between high and low pollution episodes often are

227   correlated with changes in wind direction and intensity. For the low pollution periods (19th-23rd Jan

228   and 31st Jan-2nd Feb) strong westerlies brought air masses with regional influences and high b/t

229   ratios of 0.91 (0.64-1.31). The high pollution episodes (24th -25th Jan and 4th Feb) showed low wind

230   speeds resulting in shorter travel distances of the air masses and stronger local London influences

231   (up to 87%, campaign average 37%) and corresponding low b/t ratios of 0.48 (0.39-0.58).

3.4 Diurnal averages

233   Meteorological conditions can mask emission patterns, therefore diurnal averages are used to aid in

234   their identification (Figure 7). Concentrations can depend on the mixing height in the boundary

235   layer, however LIDAR measurements showed little diurnal variation in the seasonally shallow mixing

236   height (500-1000m) (Bohnenstengel et al., in review). All compounds, bar methanol, showed a

237   double rush hour peak during weekdays (07:00-10:00 and 17:00-20:00 GMT) and lower

238   concentrations with less variability on weekends (Figure 7, E - H), suggesting vehicle exhaust as a

239   major source. At MRd, rush hour peaks were less pronounced due to the continuously high daytime

240   traffic density (68002 vehicles per day; Department for Transport, 2012), which causes the road to

241   saturate for prolonged periods during the day.

242   The early morning minima (04:00 – 06:00 GMT) can be attributed to reduced human activity which

243   sharply increases during the morning rush hour peak (07:00-10:00 GMT) (Figure 7, F – H). Methanol

244   and acetone have numerous sources and longer atmospheric lifetimes resulting in no clear diurnal

245   pattern (Figure 7, A and B).

3.5 Analyses of wind direction dependence

3.5.1 Synoptic polar plots

248   Using wind speed and direction measurements from the BT tower (190 m a.g.l.), polar plots were

249   constructed for compound mixing ratios (Figure 8) using a generalized additive model (GAM) (Hastie

250   and Tibshirani, 1990; Wood, 2006) to interpolate between averaged data points in the R package

251   openair (Carslaw, 2012; Carslaw and Ropkins, 2012). At NK high concentrations for most compounds

252   were associated with low wind speeds (i.e. <5 m s^{-1}) indicating local emission sources. Methanol

253   showed high concentrations with WSW wind directions and speeds >5 m s^{-1} possibly representing

254   pollution transported to the site from a biodiesel production facility located 1km SW of the site.

255   Biodiesel production from waste cooking oil by transesterification often involves evaporating

256   methanol.

257 At MRd methanol showed high concentrations with S and N winds >10 m s^{-1}, whereas benzene is
258 representative of the other compounds with patches of increased concentrations at speeds of 5-10
259 m s^{-1}. The WSW and ENE patches coincide with the directional layout of Marylebone Rd, while the
260 SSW source may originate from traffic in the Marble Arch/Hyde Park Corner area, which boasted the
261 highest annual mean traffic count of 100574 motor vehicles per day in all of Westminster, London
262 (DfT, 2012).

263 **3.5.2 Synoptic wind direction dependencies and comparison with NAEI**

264 To quantify wind direction dependencies (Section 3.5.1) and compare measured VOC mixing ratios at
265 MRd with the National Atmospheric Emissions Inventory (NAEI) for estimated emissions, general
266 linear models were used for each compound concentration against the four wind direction
267 categories. There was no significant difference in wind speed with direction. Correlations of VOC
268 concentrations with wind speed showed weak negative relationships ($r = -0.38$ to -0.14, $p < 0.05$)
269 indicating that a dilution effect depending on wind speed from above-canyon air mass mixing may
270 play a small role in street canyon concentrations.

271 All species showed significant differences in mixing ratios with wind direction (F- statistic 6.73 - 41.8,
272 $p < 0.001$ for measured compounds; $F = 4.48$, $p<0.01$ for estimated benzene) and agreed with the
273 polar plots. Differential source density within the four sectors and fetch variability over the city are
274 likely reasons.

275 Estimated emissions and observed concentrations for benzene agreed that low emission source
276 densities to the N resulted in low observed mixing ratios. The largest estimated emissions were to
277 the E, whereas measurements indicated the S. Regent's Park to the N and Hyde Park to the S have
278 large areas of low emissions reducing the estimates in these sectors. Emission estimates also ignore
279 background values from greater fetch across London. High localized emission sources seen in the
280 polar plots (Figure 8) could be responsible for higher measured VOC concentrations to the W and S,
281 which partially agrees with the high estimated emissions from the nearest westerly grid cell.
282 Estimated emissions from the NAEI are integrated over 1 km^2 grid resolution, but localized sub-grid
283 scale effects may be masked by the grid averaging area. It must be emphasized that the volume
284 mixing ratios were measured at ground-level within the street canyon, whereas the wind data are
285 representative of synoptic winds above the street canyons.

286 **4 Conclusion**

287 High VOC concentrations during the winter in urban locations are mostly from traffic emissions. This
288 was reflected at both sites in diurnal profiles, VOC/VOC and VOC/CO correlations and ratios, wind
289 sector dependence analyses and polar plots. Measurements at the NK background site indicated

290 significantly lower mixing ratios than at the MRd kerbside site, even though AHN data showed that
291 kerbside concentrations were higher during the first measurement period, suggesting site
292 differences due to the location with different source strengths and proximity.

293 Comparison of PTR-MS and GC-FID data from MRd for aromatics showed good correlation and
294 qualitative agreement. However, PTR-MS data were significantly higher possibly due to some
295 isobaric interference from additional compounds and fragments, and possibly systematic errors
296 introduced during instrument background corrections. Short term variations in the ratio of traffic
297 related compounds from differences in traffic density, driving style, vehicle and fuel types were
298 observed by PTR-MS at MRd site and higher correlations with CO for PTR-MS than the GC-FID
299 measurements were likely due to the fast response and longer sampling times of the PTR-MS. The
300 AHN can only report hourly arithmetic means due to the methods employed, possibly leading to a
301 reporting bias and a loss of information on short term variability.

302 Elevated concentrations were mostly observed when synoptic-scale wind speeds were low at NK as
303 dispersion of localised emissions was reduced. However, some non-local emission sources were
304 detected using polar plots and possible sources were identified. There were significant differences in
305 VOC concentrations with wind direction. When compared with estimated benzene emissions by the
306 NAEI, estimates were less representative when VOC concentrations were high, as they are unable to
307 capture the influence of city background emissions and reduced local sub-grid emission source
308 contributions.

Acknowledgements

References

318 **References**

319 Atkinson, R. (2000). Atmospheric chemistry of VOCs and NOx. Atmospheric Environment, 34(12-14),
320 2063–2101, doi:10.1016/S1352-2310(99)00460-4.

321 Baker, A. K., Beyersdorf, A. J., Doezema, L. A., Katzenstein, A., Meinardi, S., Simpson, I. J., Blake, D. R.
322 & Rowland, F. S. (2008). Measurements of nonmethane hydrocarbons in 28 United States cities.
323 Atmospheric Environment, 42(1), 170–182, doi:10.1016/j.atmosenv.2007.09.007,.

324 Bohnenstengel, S.I., Belcher, S.E., Allan, J.D., Allen, G., Bacak, A., Bannan, T.J., Barlow, J.F., Beddows,
325 D. C. S., Bloss, W. J., Booth, A. M., Chemel, C., Coceal, O., Di Marco, C.F., Faloon, K. H., Fleming, Z.,
326 Furger, M., Geitl, J. K., Graves, R. R., Green, D. C., Grimmond, C. S. B., Halios, C., Hamilton, J. F.,
327 Harrison, R. M., Heal, M. R., Heard, D. E., Helfter, C., Herndon, S. C., Holmes, R. E., Hopkins, J. R.,
328 Jones, A. M., Kelly, F. J., Kotthaus, S., Langford, B., Lee, J. D., Leigh, R. J., Lewis, A. C., Lidster, R. T.,
329 Lopez-Hilfiker, F. D., McQuaid, J. B., Mohr, C., Monks, P. S., Nemitz, E., Ng, N. L., Percival, C. J.,
330 Prévôt, A. S. H., Ricketts, H. M. A., Sokhi, R., Stone, D., Thornton, J. A., Tremper, A. H., Valach, A. C.,
331 Visser, S., Whalley, L. K., Williams, L. R., Xu, L., Young, D. E. & Zotter, P. (submitted 2013).
332 Meteorology, air quality, and health in London: The ClearfLo project. Bulletin of the American
333 Meteorological Society.

334 Borbon, A., Fontaine, H., Veillerot, M., Locoge, N., Galloo, J. C., & Guillermo, R. (2001). An
335 investigation into the traffic-related fraction of isoprene at an urban location, Atmospheric
336 Environment, 35(22), 3749-3760, doi:10.1016/S1352-2310(01)00170-4.

337 Broadway, G. & Tipler, A. (2008). Gas Chromatography: Ozone Precursor Analysis Using a Thermal
338 Desorption- GC System (White paper), 1–13.

339 Cady-Pereira, K. E., Shephard, M. W., Millet, D. B., Luo, M., Wells, K. C., Xiao, Y., Payne, V. H. &
340 Worden, J. (2012). Methanol from TES global observations: retrieval algorithm and seasonal and
341 spatial variability. Atmospheric Chemistry and Physics, 12(17), 8189–8203, doi:10.5194/acp-12-8189-
342 2012.

343 Carslaw, D.C. & Ropkins, K. (2012). openair — an R package for air quality data analysis.
344 Environmental Modelling & Software, 27-28, 52-61.

345 Carslaw, D. (2012). The openair manual — open-source tools for analysing air pollution data. Manual
346 for version 0.5-16. King's College London.

347 Chan, C., Ozkaynak, H., Spengler, J. D., & Sheldon, L. (1991). Driver Exposure to Volatile Organic
348 Compounds , CO , Ozone , and NO , under Different Driving Conditions. Environmental Science &
349 Technology, (5), 964–972.

350 Chan, C. Y., Chan, L. Y., Wang, X. M., Liu, Y. M., Lee, S. C., Zou, S. C., Sheng, G. Y. & Fu, J. M. (2002).
351 Volatile organic compounds in roadside microenvironments of metropolitan Hong Kong,
352 Atmospheric Environment 36, 2039–2047.

353 de Gouw, J. A., Middlebrook, A. M., Warneke, C., Goldan, P. D., Kuster, W.C., Roberts, J. M.,
354 Fehsenfeld, F. C., Worsnop,D. R., Canagaratna, M. R., Pszenny, A. A. P., Keene, W. C.,Marchewka, M.,
355 Bertman, S. B., & Bates, T. S. (2005). Budget of organic carbon in a polluted atmosphere: Results
356 from the New England Air Quality Study in 2002. Journal of Geophysical Research, 110, D16305.

10

357 de Gouw, J. & Warneke, C. (2007). Measurements of volatile organic compounds in the Earth's
358 atmosphere using proton-transfer-reaction mass spectrometry. Mass Spectrometry Reviews, 26,
359 223– 257, doi:10.1002/mas.

360 Department for Transport, www.dft.gov.uk/traffic-counts/, accessed on 22/11/2013.

361 Derwent, R. G. (1995). Sources, Distributions, and Fates of VOCs in the Atmosphere, (23).

362 Erickson, M. H., Gueneron, M. & Jobson, B. T. (2014). Measuring long chain alkanes in diesel engine
363 exhaust by thermal desorption PTR-MS, Atmospheric Measurement Techniques, 7(1), 225-239,
364 doi:10.5194/amt-7-225-2014.

365 Hastie, T. J. & Tibshirani, R. (1990). Generalized additive models. Chapman and Hall, London.

366 Heeb, N. V, Forss, A., Bach, C., Reimann, S., Herzog, A., & Jäckle, H. W. (2000). A comparison of
367 benzene , toluene and C_2 -benzenes mixing ratios in automotive exhaust and in the suburban
368 atmosphere during the introduction of catalytic converter technology to the Swiss Car Fleet.
369 Atmospheric Environment, 34, 3103–3116.

370 Hewitt, C. N., Hayward, S., & Tani, A. (2003). The application of proton transfer reaction-mass
371 spectrometry (PTR-MS) to the monitoring and analysis of volatile organic compounds in the
372 atmosphere. Journal of Environmental Monitoring, 5(1), 1–7. doi:10.1039/b204712h

373 Hewitt, C. N. (1999). Reactive Hydrocarbons in the Atmosphere. Elsevier, New York.

374 Holzinger, R., Jordan, A., & Hansel, A. (2001). Automobile Emissions of Acetonitrile : Assessment of
375 its Contribution to the Global Source, Journal of Atmospheric Chemistry, 38, 187–193.

376 Jobson, B. T., Volkamer, R. A., Velasco, E., Allwine, G., Westberg, H., Lamb, B. K., Alexander, M. L.,
377 Berkowitz, C. M. & Molina, L. T. (2010). Comparison of aromatic hydrocarbon measurements made
378 by PTR-MS, DOAS and GC-FID during the MCMA 2003 Field Experiment. Atmospheric Chemistry and
379 Physics, 10(4), 1989–2005, doi:10.5194/acp-10-1989-2010.

380 Jones, A.R., Thomson, D.J., Hort, M. & Devenish, B. (2007). The U.K. Met Office's next-generation
381 atmospheric dispersion model, NAME III. In B. C. A.-L., Air Pollution Modeling and its Application
382 XVII: Proceedings of the 27th NATO/CCMS International Technical Meeting on Air Pollution
383 Modelling and its Application (pp. 580-589). Springer.

384 Kansal, A. (2009). Sources and reactivity of NMHCs and VOCs in the atmosphere: a review. Journal of
385 Hazardous Materials, 166(1), 17–26. doi:10.1016/j.jhazmat.2008.11.048

386 Kato, S., Miyakawa, Y., Kaneko, T. & Kajii, Y. (2004). Urban air measurements using PTR-MS in Tokyo
387 area and comparison with GC-FID measurements, International Journal of Mass Spectrometry, 235
388 (2), 103-110, doi:10.1016/j.ijms.2004.03.013

389 Kim, Y. M., Harrad, S., & Harrison, R. M. (2001). Concentrations and sources of VOCs in urban
390 domestic and public microenvironments. Environmental Science & Technology, 35(6), 997–1004.

391 Kuster, W. C., Jobson, B. T., Karl, T., Riemer, D., Apel, E., & Goldan, P. D. (2004). Intercomparison of
392 Volatile Organic Carbon Measurement Techniques and Data at La Porte during the TexAQS2000 Air
393 Quality Study, Environmental Science & Technology, 38(1), 221–228.

394 Langford, B., Davison, B., Nemitz, E., & Hewitt, C. N. (2009). Mixing ratios and eddy covariance flux
395 measurements of volatile organic compounds from an urban canopy (Manchester, UK). Atmospheric
396 Chemistry and Physics, 9, 1971–1987.

397 Langford, B., Misztal, P. K., Nemitz, E., Davison, B., Helfter, C., Pugh, T. A. M., MacKenzie, A. R., Lim,
398 S. F. & Hewitt, C. N. (2010a). Fluxes and concentrations of volatile organic compounds from a South-
399 East Asian tropical rainforest. Atmospheric Chemistry and Physics, 10(17), 8391–8412,
400 doi:10.5194/acp-10-8391-2010

401 Langford, B., Nemitz, E., House, E., Phillips, G. J., Famulari, D., Davison, B., Hopkins, J. R., Lewis, A. C.
402 & Hewitt, C. N. (2010b). Fluxes and concentrations of volatile organic compounds above central
403 London, UK. Atmospheric Chemistry and Physics, 10, 627–645.

404 Lindinger, W., Hansel, A., & Jordan, A. (1998). On-line monitoring of VOCs at pptv levels by means of
405 PTR-MS. Medical applications, food control and environmental research. International Journal of
406 Mass Spectrometry and Ion Processes, 173(7), 191–241, doi:10.1016/0015-1882(95)90197-3.

407 Maleknia, S. D., Bell, T. L., & Adams, M. A. (2007). PTR-MS analysis of reference and plant-emitted
408 volatile organic compounds. International Journal of Mass Spectrometry, 262(3), 203–210,
409 doi:10.1016/j.ijms.2006.11.010.

410 Reissell, A., Harry, C., Aschmann, S. M., Atkinson, R., & Arey, J. (1999). Formation of acetone from
411 the OH radical- and O3-initiated reactions of a series of monoterpenes. Journal of Geophysical
412 Research, 104, 13869–13879.

413 Park, C., Schade, G. W., & Boedeker, I. (2011). Characteristics of the flux of isoprene and its oxidation
414 products in an urban area. Journal of Geophysical Research: Atmospheres (1984–2012), 116(D21).

415 Spaněl, P. & Smith, D. (2000). Influence of water vapour on selected ion flow tube mass
416 spectrometric analyses of trace gases in humid air and breath. Rapid communications in mass
417 spectrometry : RCM, 14(20), 1898–906, doi:10.1002/1097-0231(20001030)14:20<1898::AID-
418 RCM110>3.0.CO;2-G.

419 UK Met Office, http://www.metoffice.gov.uk/, accessed 10/2/2012.

420 Warneke, C., de Gouw, J. A., Kuster, W. C., Goldan, P. D., & Fall, R. (2003). Validation of atmospheric
421 VOC measurements by proton-transfer-reaction mass spectrometry using a gas-chromatographic
422 preseparation method. Environmental Science & Technology, 37(11), 2494–501.

423 Warneke, C., Karl, T., Judmaier, H., Hansel, A., Jordan, A.,Lindinger, W., & Crutzen, P. J. (1999).
424 Acetone, methanol, and other partially oxidized volatile organic emissions from dead plant matter by
425 abiological processes: Significance for atmospheric HOx chemistry. Global Biogeochemical Cycles, 13,
426 9–17.

427 Warneke, C., van der Veen, C., de Gouw, J. A., & Kok, A. (2001). Measurements of benzene and
428 toluene in ambient air using proton-transfer-reaction mass spectrometry : calibration , humidity
429 dependence , and field intercomparison, International Journal of Mass Spectrometry, 207, 167–182.

430 Wood, S. (2006). Generalized Additive Models: An introduction with R. Chapman & Hall/CRC.

431 Yardley, R., Dernie, J., & Dumitrean, P. (2012). UK Hydrocarbon Network Annual Report for 2011, (1).

432   Yuan, B., Warneke, C., Shao, M. & de Gouw, J. (2014). Interpretation of volatile organic compound

433   measurements by proton-transfer-reaction mass spectrometry over the Deepwater Horizon oil spill,

434   International Journal of Mass Spectrometry, 358, 43-48.

435

436 **Figure 1.** *Top*: 5 min means of ambient air temperature (°C) and relative humidity (%) during the

437 campaign 16th Jan – 7th Feb 2012. *Bottom*: Frequency plots of mesoscale wind direction (%) with

438 subcategories of wind speed (m s^{-1}) using 30 min mean data from the WXT520 (Vaisala Ltd) at 190m

439 on the BT tower at NK (16th – 25th Jan 2012) (*left*) and MRd (25th Jan – 7th Feb 2012) (*right*).

440 **Figure 2.** 5min mean (grey) and 25 min means (black) with detection limits (dashed line) for all

441 measured VOCs (ppb) at **(a)** North Kensington and **(b)** Marylebone Rd (16th Jan – 7th Feb 2012). *M/z*

442 are 33 (methanol), 42 (acetonitrile), 45 (acetaldehyde), 59 (acetone), 69 (cycloalkanes/isoprene), 79

443 (benzene), 93 (toluene), 107 (C_2-benzenes) and 121 (C_3-benzenes).

444 **Figure 3.** 1h means for benzene, toluene, C_2- and C_3-benzenes mixing ratios (ppb) measured by the

445 PTR-MS (solid line) and GC-FID (dashed line) at Marylebone Road (25th Jan – 7th Feb 2012).

446 **Figure 4.** Scatter plots of 1h mean VOC concentrations (ppb) (benzene, toluene, C_2- and C_3-benzenes)

447 of PTR-MS against GC-FID measurements at Marylebone Road (25th Jan – 7th Feb 2012) with reduced

448 major axis (RMA) linear regressions, ± 99th confidence intervals, 1:1 line (dotted) with r-values.

449 **Figure 5.** Scatter plots of representative VOC correlations measured at North Kensington (left) and

450 Marylebone Rd (right) (16th Jan – 7th Feb 2012) using 5 min means (ppbv) with ambient air

451 temperature (°C) at time of sampling (colour bar).

452 **Figure 6.** 24 hour back trajectories from the Met Office NAME dispersion model at North Kensington

453 (16th Jan-7th Feb 2012). Daily release for 3 hours from midday (20 m height) tracking the surface

454 layer only (0-100m) for the 24 hours prior. Reproduced with permission from Zoë Fleming (NCAS,

455 University of Leicester).

456 **Figure 7.** Diurnal plots of 25min averages (ppb) for representative VOCs at North Kensington and

457 Marylebone Road (16th Jan – 7th Feb 2012) with the 95% confidence interval (shaded areas), all days

458 (solid line), weekdays (dashed line) and weekends (dotted line).

459 **Figure 8.** Representative selection of polar plots of synoptic wind speed (m s^{-1}) against wind

460 direction (°) from the BT tower (190m) with VOC mixing ratios (ppb) as a third variable (colour bar)

461 for methanol (*m/z* 33), acetonitrile (*m/z* 42) and benzene (*m/z* 79) at North Kensington (16th -25th Jan

462 2012) (*top*) and Marylebone Rd (25th Jan – 7th Feb 2012) (*bottom*).

14

463

464 **Table 1a. Summary of 5 min averages of VOC mixing ratios (ppb) at North Kensington, London (16th - 25th Jan 2012).**

Mixing ratios (ppb)	Methanol m/z 33	Aceto-nitrile m/z 42	Acetal-dehyde m/z 45	Acetone m/z 59	Cycloalkanes/ Isoprene m/z 69	Benzene m/z 79	Toluene* m/z 93	C_2-benzenes m/z 107	C_3-benzenes m/z 121
Lifetime (OH[a])	12 d	1.5 yr	8.8 h	53 d	1.4 h	9.4 d	1.9 d	5.9 h[b]	4.3 h[c]
N	2219	2202	2211	2213	2199	2227	2226	2225	2226
LoD	0.37	0.04	0.18	0.06	0.005	0.04	0.01	0.08	0.03
Min.	2.86	<LoD	<LoD	0.37	<LoD	<LoD	0.03	<LoD	0.04
1st quartile	5.06	0.05	0.29	0.95	0.08	0.14	0.21	0.23	0.24
Median	5.77	0.06	0.46	1.16	0.14	0.24	0.42	0.44	0.37
Geom. mean	6.17	0.07	0.50	1.25	0.13	0.24	0.42	0.45	0.40
Arithm. mean	6.40	0.08	0.62	1.34	0.17	0.31	0.60	0.63	0.50
3rd quartile	8.00	0.07	0.75	1.51	0.21	0.39	0.74	0.79	0.59
Max.	10.4	0.10	3.67	6.79	0.98	2.13	4.92	4.89	3.65
SD	1.84	0.05	0.51	0.67	0.13	0.26	0.61	0.62	0.42
Skew	0.39	2.09	2.08	3.02	1.90	2.19	2.53	2.62	2.61
Kurtosis	-0.89	6.03	5.25	13.5	4.85	6.96	8.71	9.45	9.36

465 [a] Atmospheric lifetimes with regard to OH for a 12-h daytime average OH radical concentration of 2.0×10^6
466 molecule cm^{-3} (Atkinson, 2000).
467 [b] example using m-xylene.
468 [c] example using 1,2,4-trimethylbenzene.

469

470 **Table 1b. Summary of 5min averages of VOC mixing ratios (ppb) at Marylebone Rd, London (25th Jan - 7th Feb 2012).**

Mixing ratios (ppb)	Methanol m/z 33	Aceto-nitrile m/z 42	Acetal-dehyde m/z 45	Acetone m/z 59	Cycloalkanes/ Isoprene m/z 69	Benzene m/z 79	Toluene m/z 93	C_2-benzenes m/z 107	C_3-benzenes m/z 121
N	2712	2718	2716	2705	2720	2715	2713	2708	2715
LoD	0.37	0.04	0.18	0.06	0.005	0.04	0.01	0.08	0.03
Min.	1.34	0.08	0.38	0.70	0.15	0.06	0.02	<LoD	0.05
1st quartile	3.47	0.16	0.92	0.95	0.31	0.38	0.49	0.81	0.50
Median	5.00	0.19	1.34	1.15	0.39	0.56	0.80	1.21	0.86
Geom. mean	4.48	0.19	1.39	1.20	0.41	0.55	0.85	1.21	0.85
Arithm. mean	4.67	0.20	1.61	1.25	0.44	0.63	1.18	1.45	1.11
3rd quartile	5.61	0.24	2.07	1.47	0.53	0.81	1.50	1.87	1.52
Max.	7.39	0.56	6.18	3.78	1.18	3.57	10.0	7.60	4.76
SD	1.27	0.07	0.92	0.38	0.17	0.35	1.13	0.9	0.79
Skew	-0.47	1.33	1.29	1.21	1.05	1.68	2.8	1.62	1.21
Kurtosis	-0.72	2.28	1.53	2.04	0.65	5.36	11.6	0.02	1.20

471
472

16

473 **Table 2 Summary of 1h averages of compounds (ppb) measured by both PTR-MS and GC-FID at Marylebone Rd, London**
474 **(25th Jan – 7th Feb 2012).**

Mixing ratios (ppb)	PTR-MS				GC-FID			
	Benzene m/z 79	Toluene m/z 93	C_2-benzenes m/z 107	C_3-benzenes m/z 121	Benzene m/z 79	Toluene m/z 93	C_2-benzenes m/z 107	C_3-benzenes m/z 121
N	274	274	274	256	302	302	302	302
LoD	*0.04*	*0.01*	*0.08*	*0.03*	*0.01*	*0.01*	*0.01*	*0.01*
Min.	0.17	0.13	0.29	0.13	0.14	0.07	0.03	0.01
1st quartile	0.39	0.52	0.87	0.46	0.30	0.38	0.57	0.13
Median	0.57	0.82	1.23	0.91	0.42	0.61	0.83	0.24
Geom. mean	0.58	0.95	1.30	0.81	0.41	0.66	0.86	0.24
Arithm. mean	0.63	1.17	1.44	1.07	0.47	0.87	1.01	0.33
3rd quartile	0.82	1.53	1.89	1.51	0.58	1.09	1.32	0.46
Max.	2.26	6.42	5.12	3.71	1.42	5.17	4.51	1.45
SD	0.32	1.01	0.81	0.74	0.23	0.83	0.63	0.29
Skew	1.30	2.06	1.38	0.93	1.53	2.33	1.39	1.27
Kurtosis	2.65	5.21	2.53	0.39	2.98	6.36	2.13	1.16

475

476

17

477 **Table 3. Mean VOC/CO ratios for volume mixing ratios (ppbv/ppbv) at NK and MRd, London (16th Jan - 7th Feb 2012).**

Compound	ClearfLo					
	NK[a]		MRd			
	PTR-MS		PTR-MS[b]		GC-FID[c]	
	[VOC]/[CO]	r	[VOC]/[CO]	r	[VOC]/[CO]	r
Methanol	2.13E-02	0.28	1.20E-02	0.27		
Acetonitrile	2.70E-04	0.87	5.21E-04	0.55		
Acetaldehyde	2.14E-03	0.93	4.14E-03	0.84		
Acetone	4.53E-03	0.62	3.18E-03	0.74		
Cycloalkanes/ Isoprene	5.74E-04	0.80	1.13E-03	0.82		
Benzene	1.08E-03	0.96	1.59E-03	0.75	1.58E-03	0.68
Toluene	2.07E-03	0.93	3.09E-03	0.72	3.33E-03	0.65
C2-benzenes	2.16E-03	0.89	3.69E-03	0.66	4.70E-03	0.58
C3-benzenes	1.72E-03	0.86	2.60E-03	0.65	1.61E-03	0.68

478 [a]N = 226, [b]N =256-274, [c]N =302
479
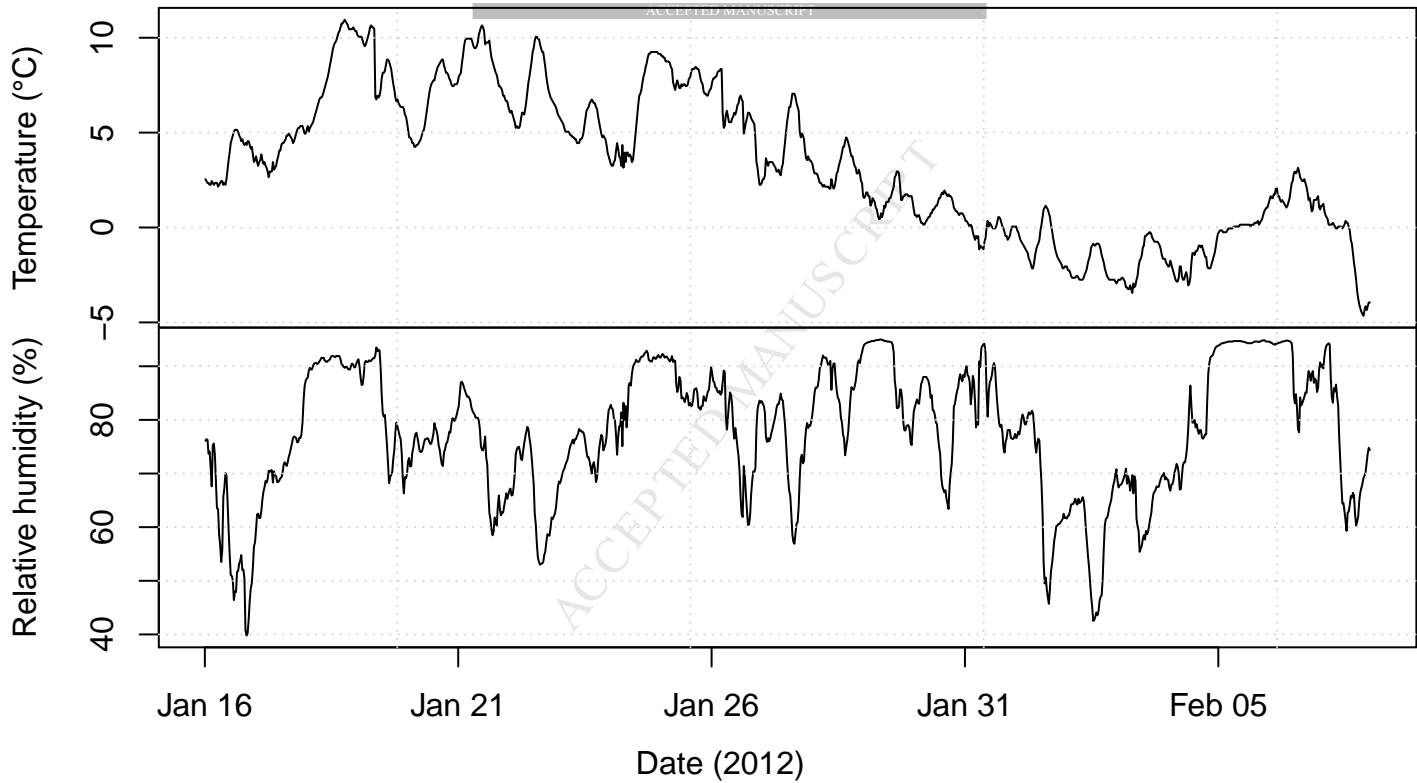
North Kensington wind frequency

	wind spd.
■	1.8–2.8
■	1.6–1.8
■	1.4–1.6
■	1.2–1.4
■	1–1.2
■	0.8–1
■	0.6–0.8
■	0.4–0.6
■	0.2–0.4
■	0.12–0.2
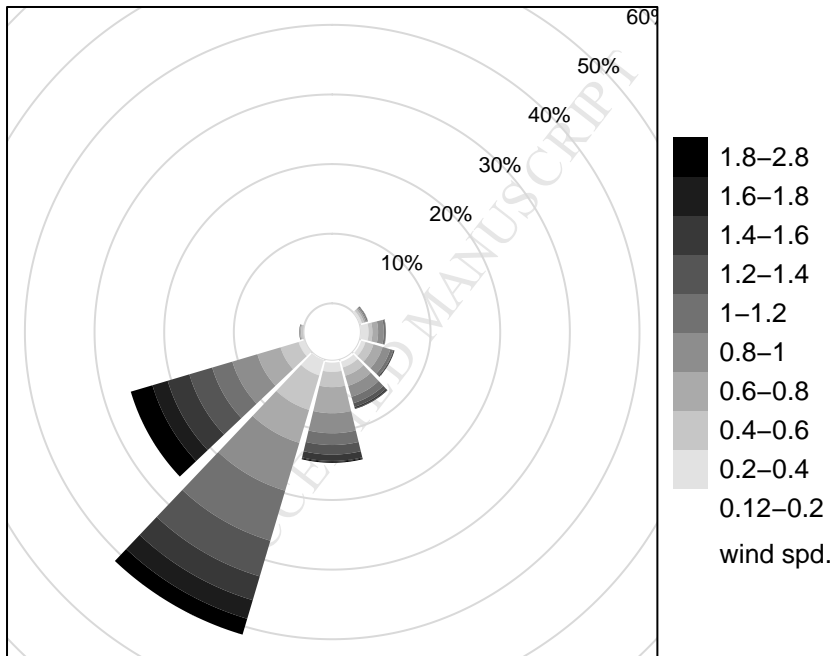
Frequency of counts by wind direction (%)

Marylebone Rd wind frequency

Frequency of counts by wind direction (%)

Date (2012)

ACCEPTED MANUSCRIPT

Benzene (m/z 79) [ppb]

m79 (PTR) = 1.38*[m79 (GC)] + 0.002
r = 0.90

PTR-MS

GC–FID

Toluene (m/z 93) [ppb]

m93 (PTR) = 1.23*[m93 (GC)] + 0.09
r = 0.91

PTR-MS

GC–FID
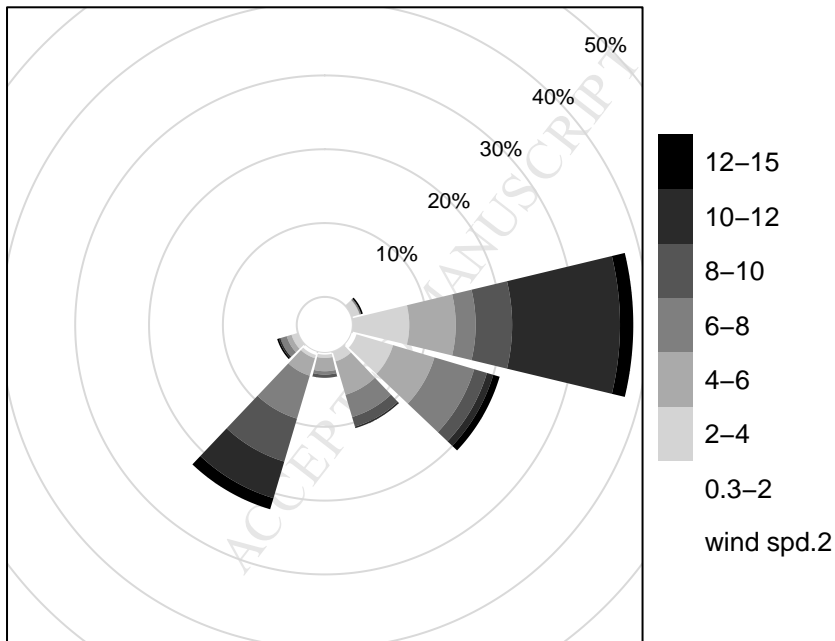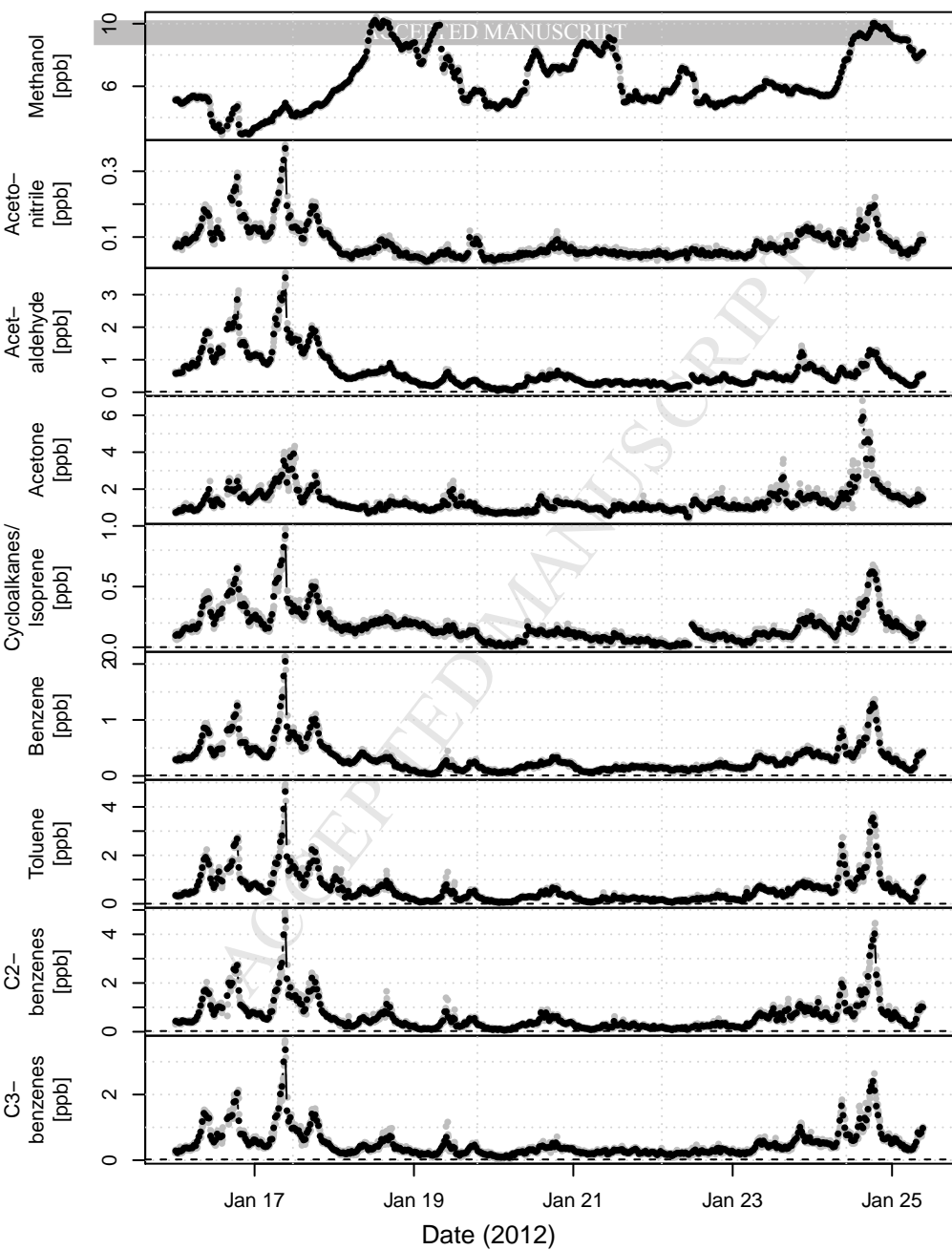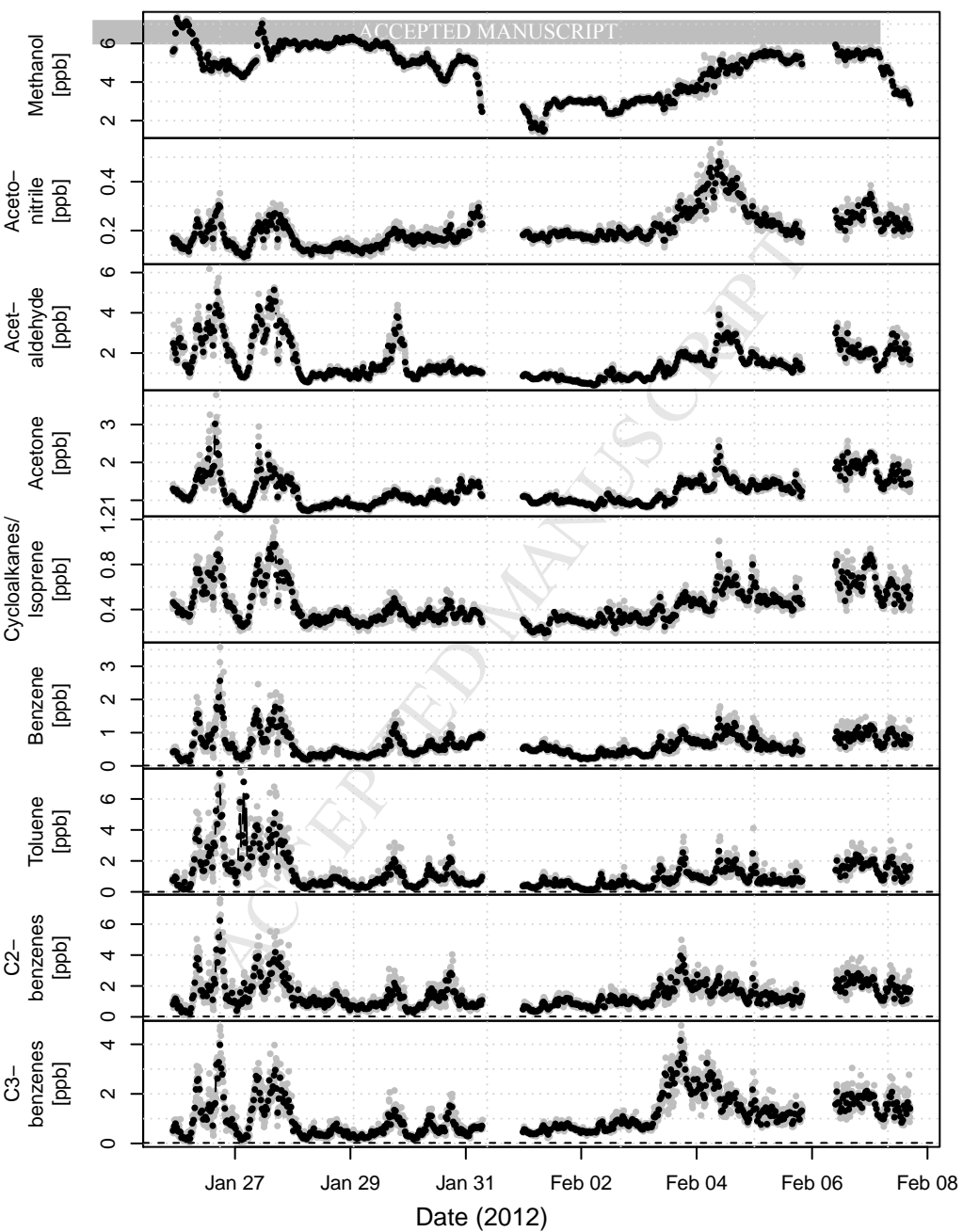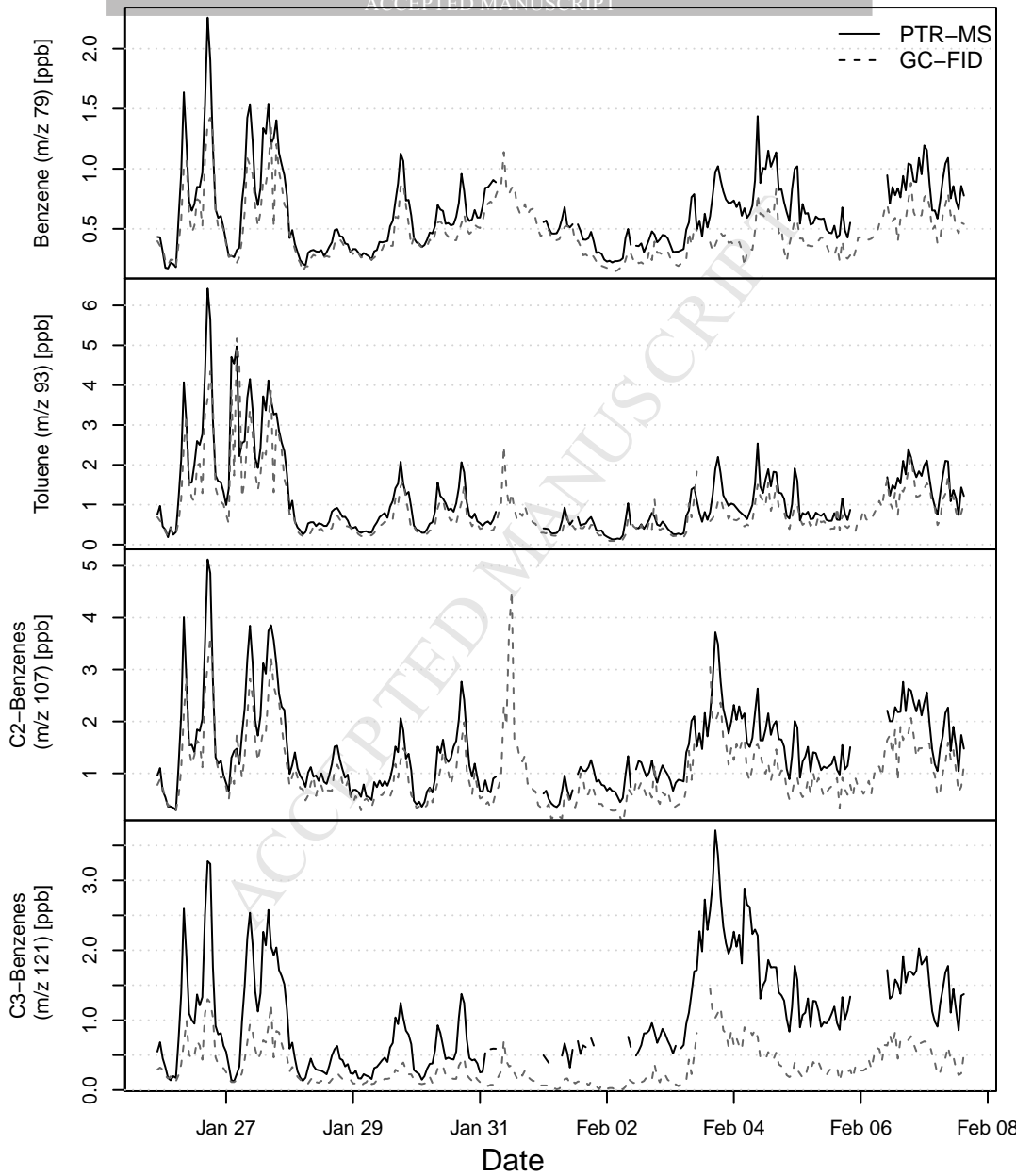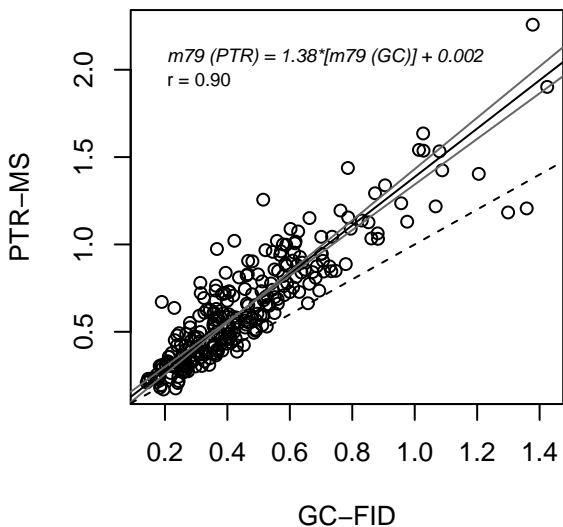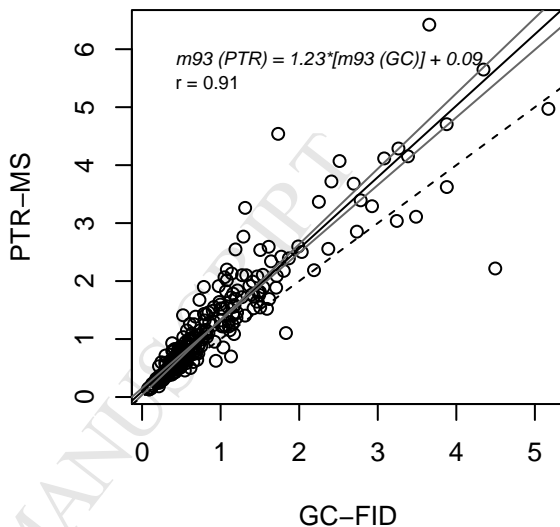
C2–Benzenes (m/z 107) [ppb]

m107 (PTR) = 1.29*[m107 (GC)] + 0.15
r = 0.91

PTR-MS

GC–FID
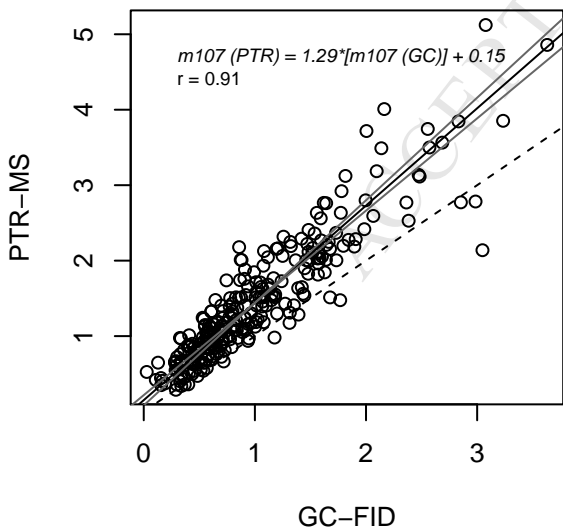
C3–Benzenes (m/z 121) [ppb]

m121 (PTR) = 2.54*[m121 (GC)] + 0.14
r = 0.91

PTR-MS

GC–FID

2012/01/21

1 day (0−100m) arriving at BT tower 3 Hourly release from: 201201211200
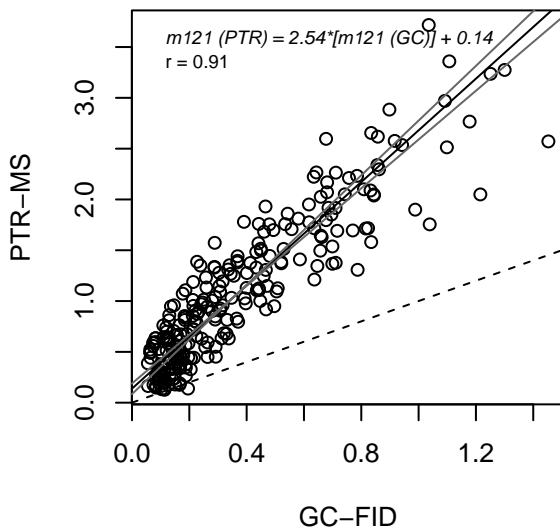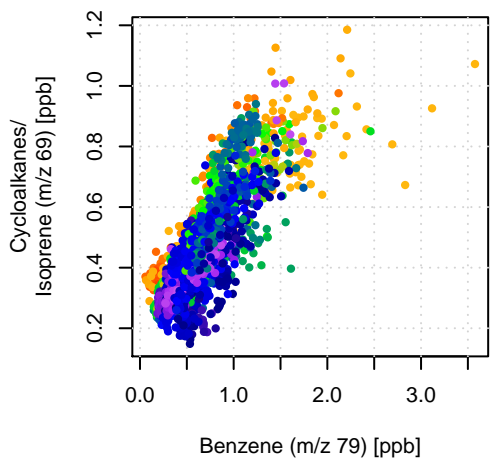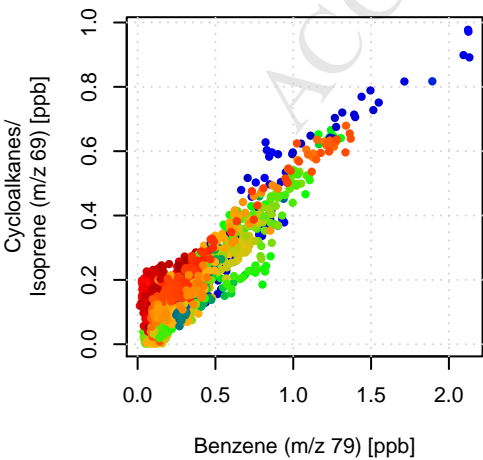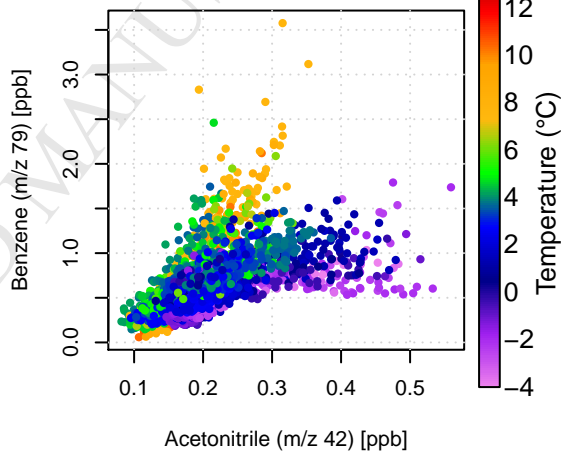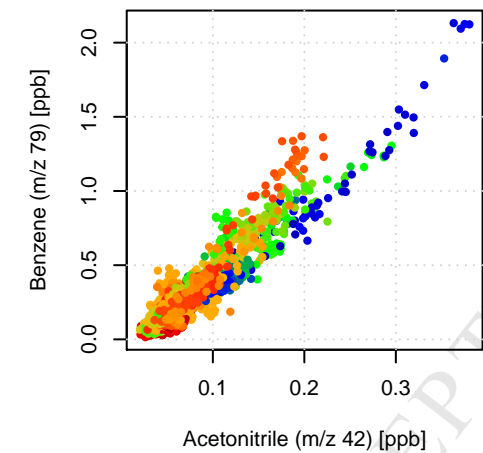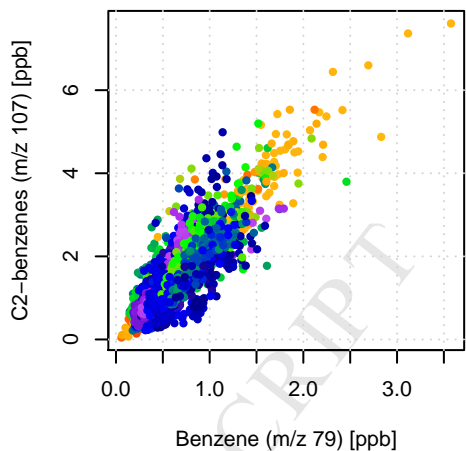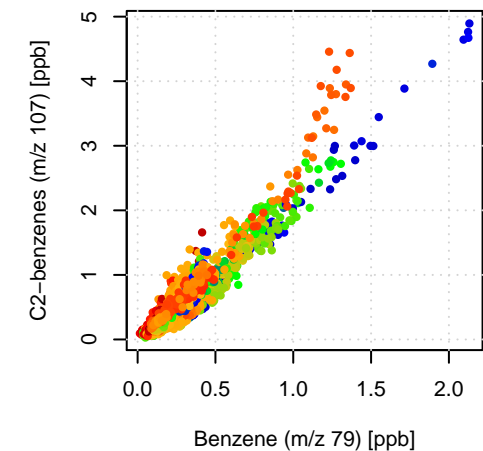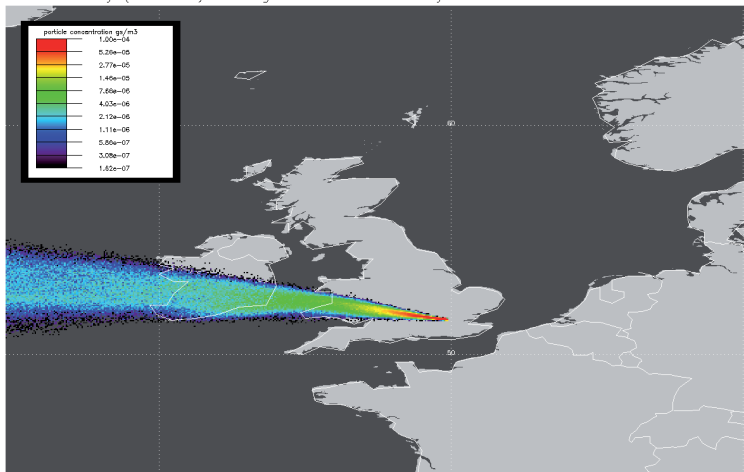
2012/01/24

1 day (0−100m) arriving at BT tower 3 Hourly release from: 201201240900
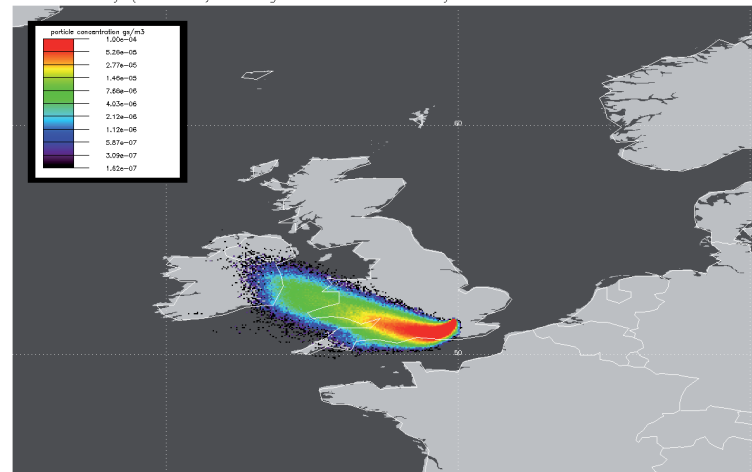
2012/02/01

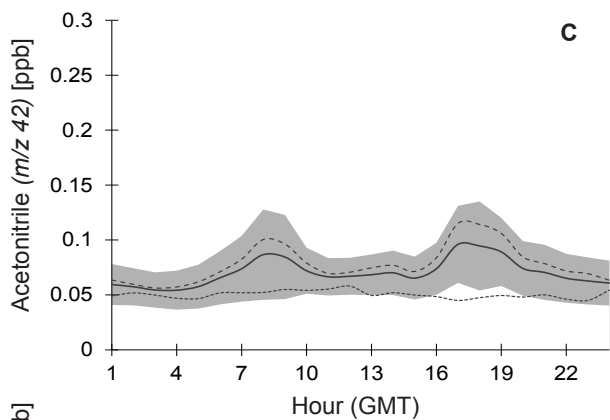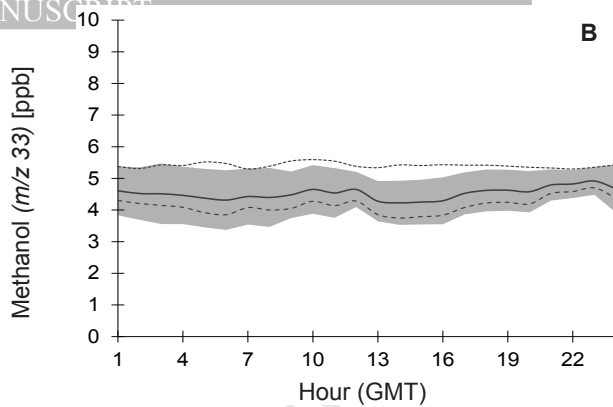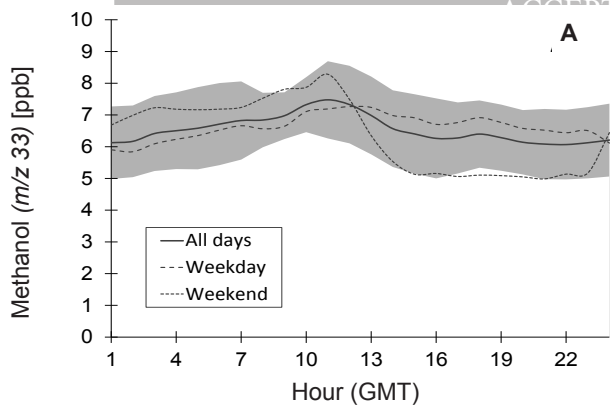1 day (0−100m) arriving at BT tower 3 Hourly release from: 201202011200
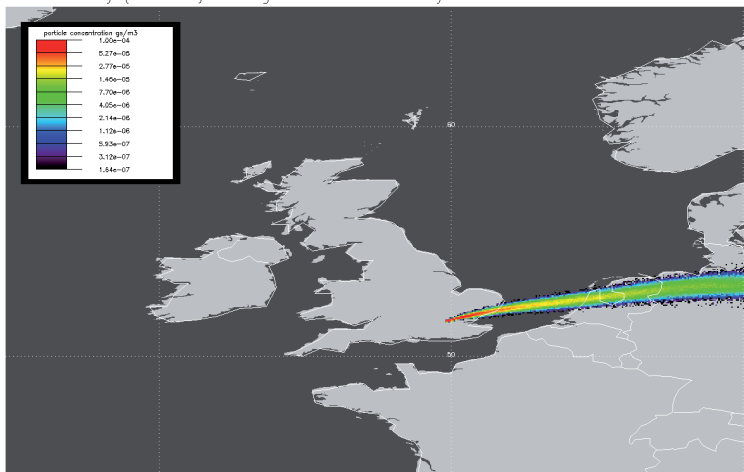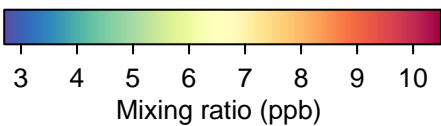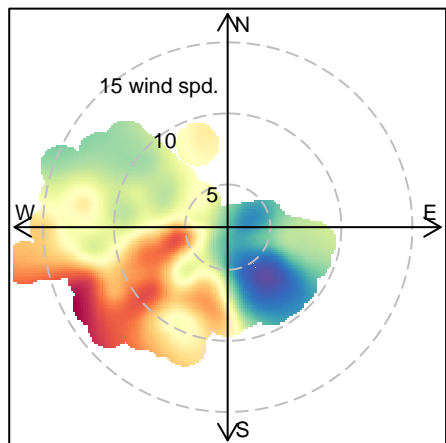
2012/02/04

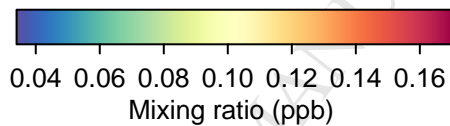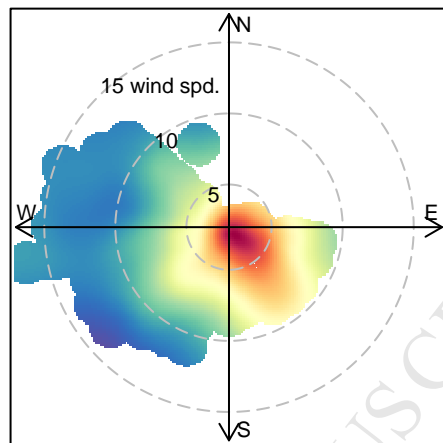1 day (0−100m) arriving at BT tower 3 Hourly release from: 201202041200
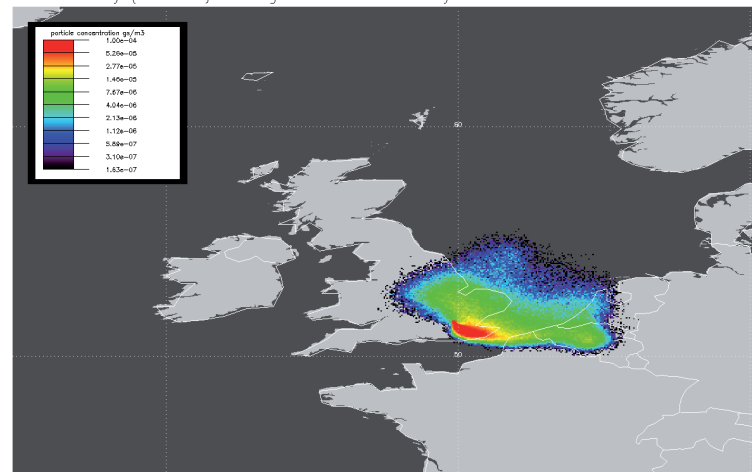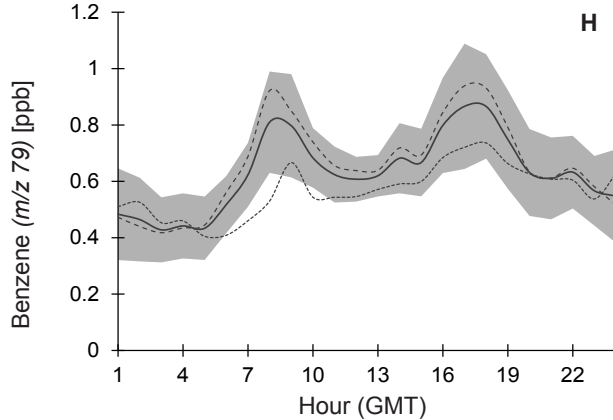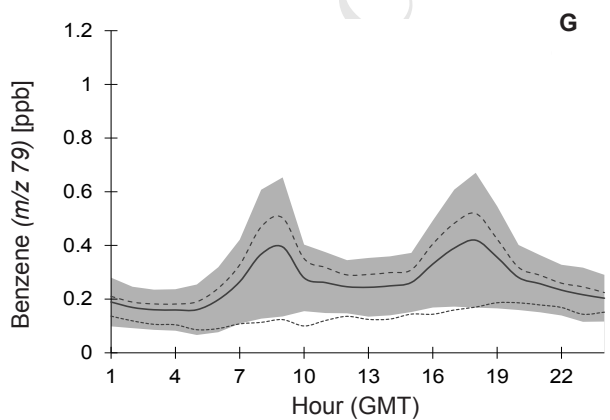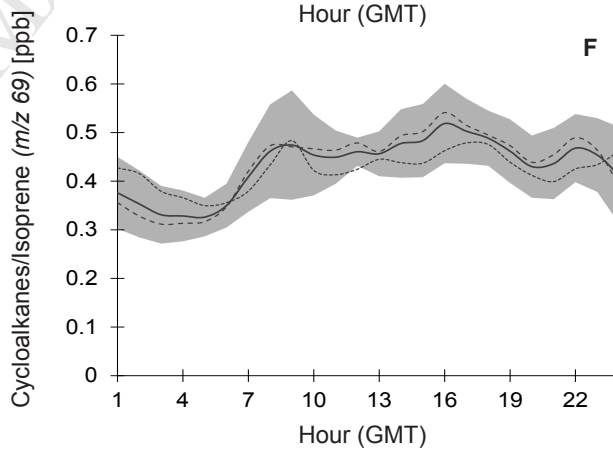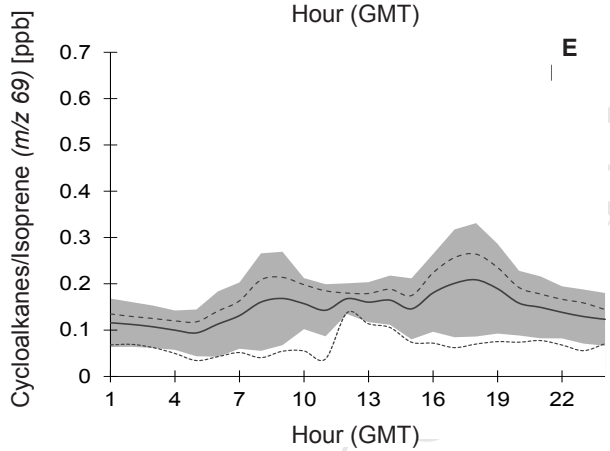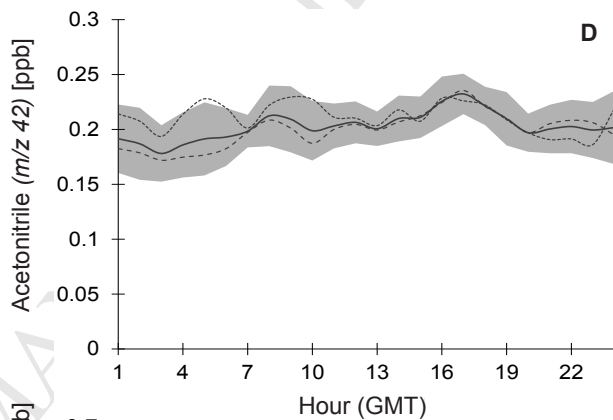
Methanol (m/z 33)   Acetonitrile (m/z 42)   Benzene (m/z 79)
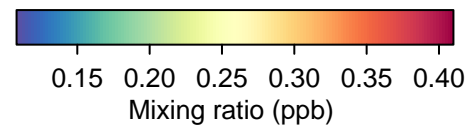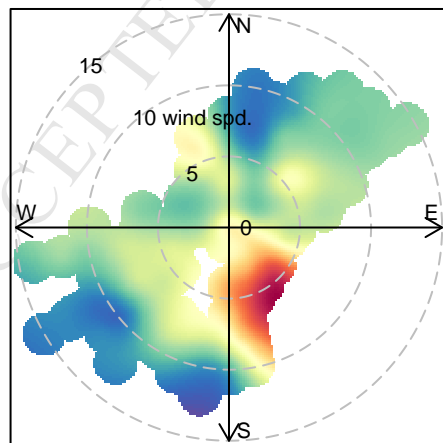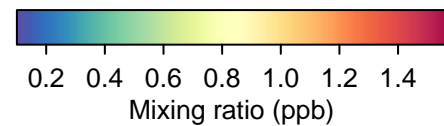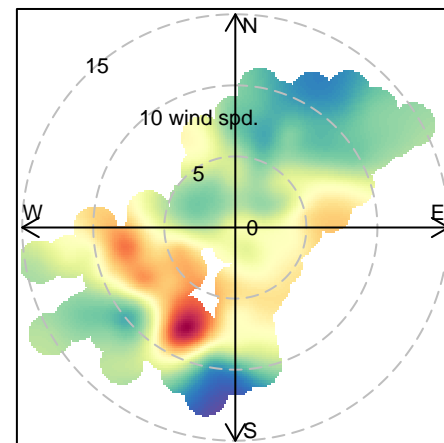
Highlights

- Volatile organic compound concentrations were measured in central London.
- Measurements were compared with the automatic hydrocarbon network.
- Vehicle emissions were the main source at both urban background and kerbside sites.
- Some effects of temperature on compound correlations were observed.
- Excellent qualitative agreement was seen between the measurement instruments.

PTR-MS: MID measurement cycle

M21	M33	M39	M42	M45	M59	M69	M79	M93	M107	M121

0   0.5   2.5   4.5   6.5   8.5   10.5   12.5   14.5   16.5   18.5   20.5   22.5

Time [sec]
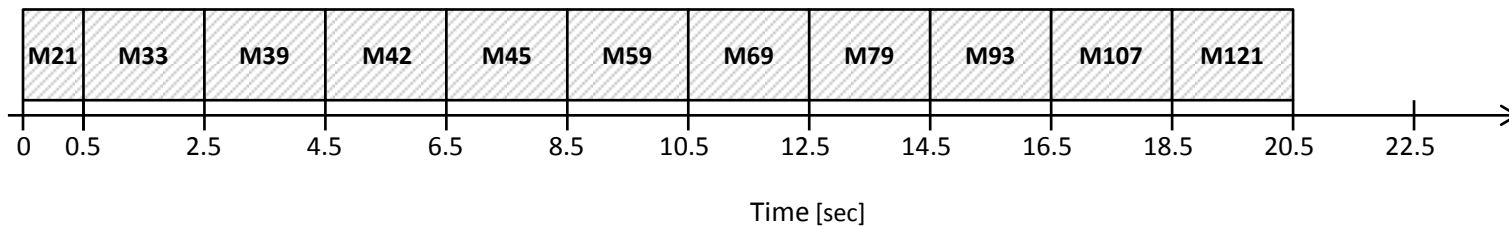
PTR-MS: 1h operating cycle

ZA	MID	SCAN	MID

0   5   30   35   60

Time [min]

GC-FID operating cycle

4a.	5a.	4b.	5b.	4c.

1b.	2b.	3b.	1c.	2c.	3c.

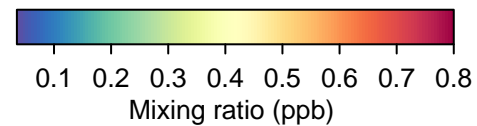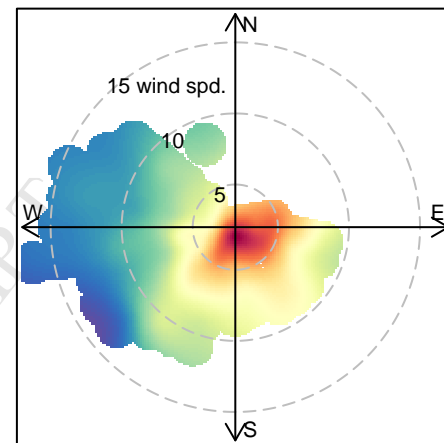0   1   2

Time [hours]

Methanol (m/z 33)

Acetonitrile (m/z 42)

Acetaldehyde (m/z 45)

Acetone (m/z 59)

Isoprene (m/z 69)

Benzene (m/z 79)

Toluene (m/z 93)

C2-benzenes (m/z 107)

C3-benzenes (m/z 121)

Normalised RH+ signal (ncps)

Mixing ratio (ppb)

m69 (PTR) = 4.6[m69 (GC)] + 0.05*
r = 0.94

PTR−MS (m/z 69) [ppb]

GC−FID Isoprene [ppb]
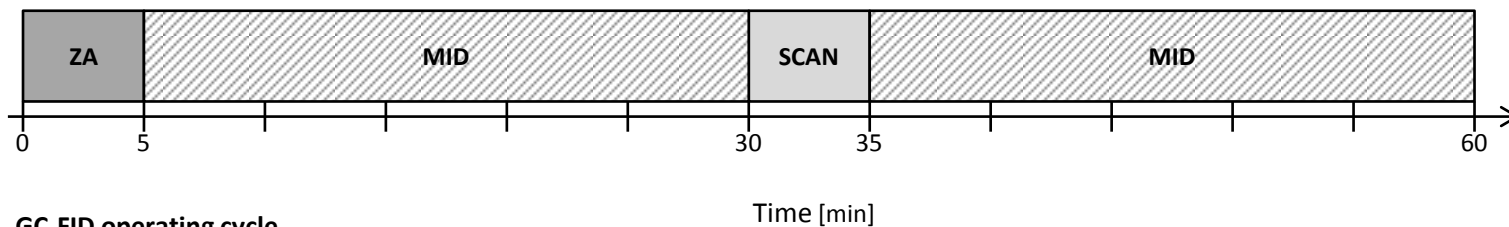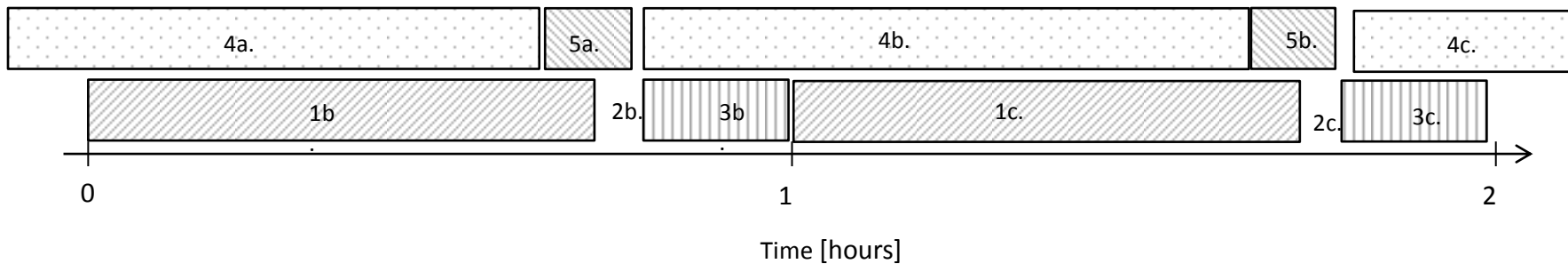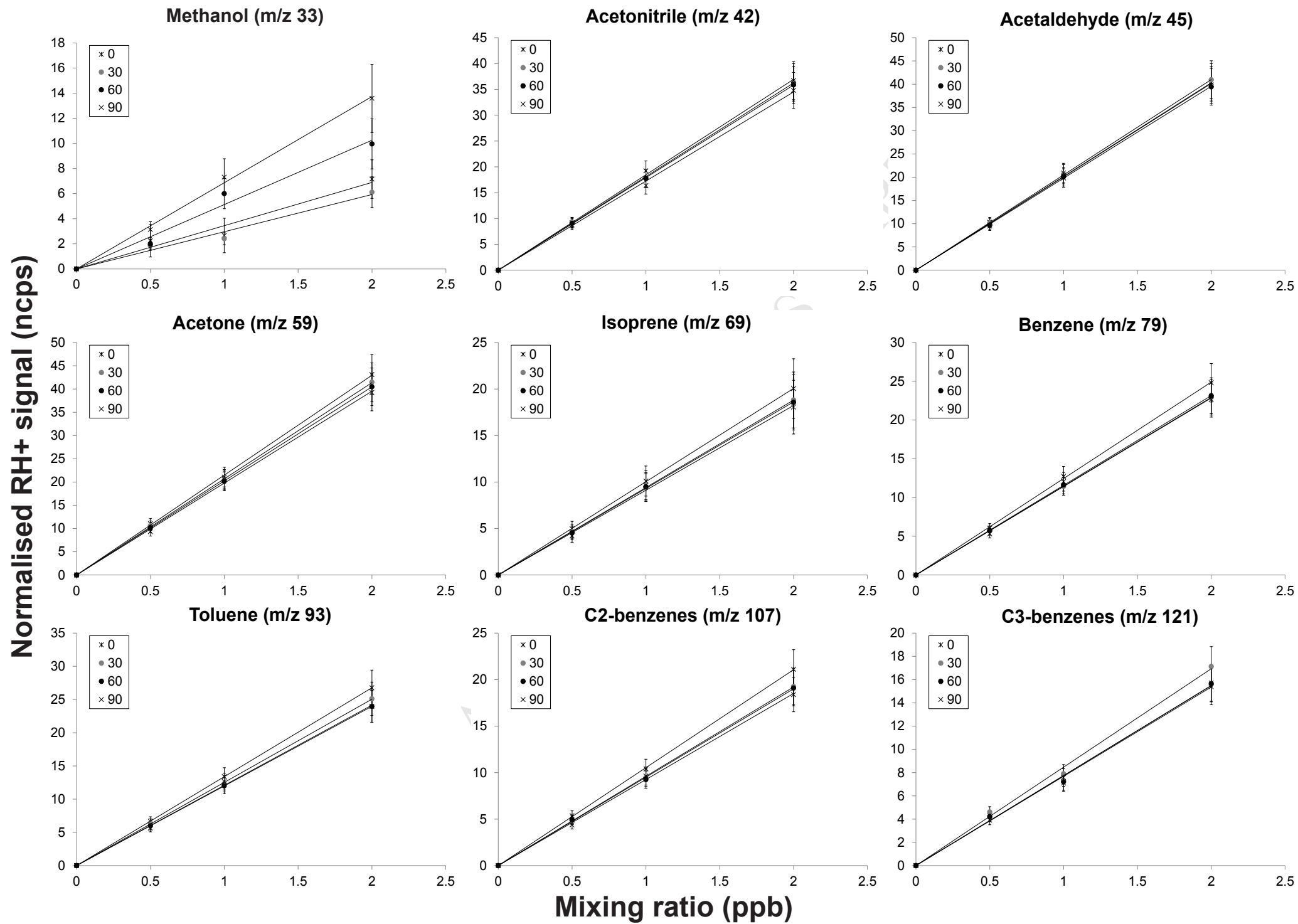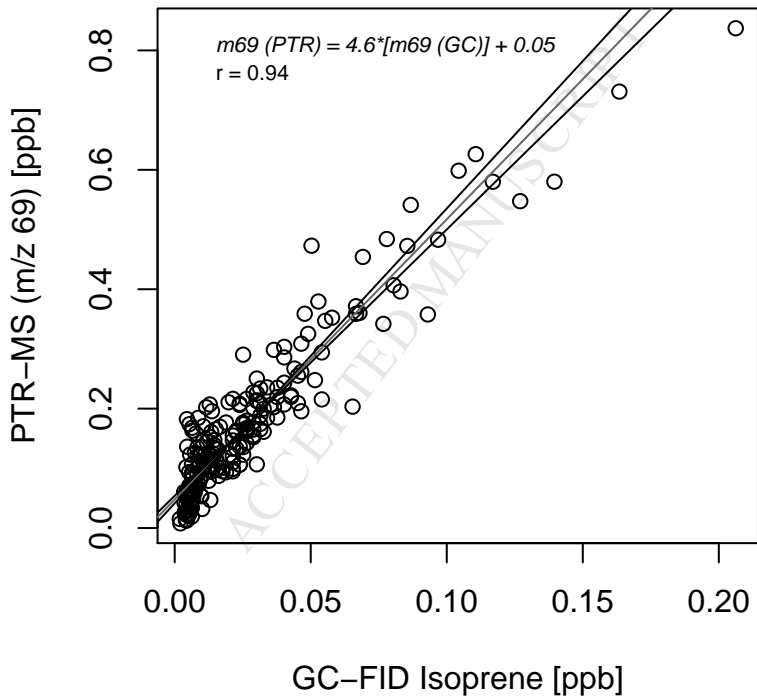
1   **Supplementary content**

2   **A. Details on measurement sites, instrument parameters and duty cycles for both**
3   **PTR-MS and GC-FID**

4   Extensive comparisons of the measurement sites and the mean meteorological
5   measurements during the two measurement periods are summarised in Table A1.

6   **A1. PTR-MS**

7   A high-sensitivity proton transfer reaction- mass spectrometer (PTR-MS) fitted with three
8   Varian turbo-molecular pumps and a 9.5 cm long drift tube was used for online
9   measurements VOC mixing ratios. During each deployment of the PTR-MS, drift tube
10   pressure, temperature and voltage were kept constant at 2.06 mbar, 48 °C and 550 V
11   respectively to maintain an E/N ratio of 125 Td. Air was subsampled from the main line with
12   an inlet flow rate of 0.25-0.3 l min^{-1}. The primary ion count (m/z 19) ranged between 6 - 14 x
13   10^6 cps with a mean of 11 x 10^6 cps. The $H_3O^+.H_2O^+$ water cluster ions ranged between 6.5 x
14   10^4 – 2.6 x 10^5 cps with a mean of 1.4 x 10^5 cps which represented on average 1.7% of the
15   primary ion signal, while the O_2+ signal (m/z 32) was <2% of the primary ion signal. The 1 h
16   measurement protocol consisted of 5 min zero air measurements using a zero air generator
17   (Parker Balston, UK), then 25 min MID mode, followed by 5 min mass scans and another 25
18   min in MID mode (Figure A1). During the MID mode, 11 selected masses were measured
19   with a dwell time of 2 s per mass and 0.5 s for the primary ion, resulting in a 20.5 s cycle
20   time, whereas SCAN modes cycled through the mass range m/z 21 – 206 with a dwell time
21   of 0.5 s each.

22   **A2. GC-FID**

23   The GC-FID method used by the AHN has recently been linked to the QA/QC procedures of
24   the EU Infrastructure Project ACTRIS (www.actris.net). The method includes a TurboMatrix
25   thermal desorption (TD) unit with an online sampling accessory to gather samples directly
26   from ambient air. The TD extracts the compounds onto an adsorbent trap, which is cooled to
27   -30°C. The analytes are then thermally desorbed and transported through a heated transfer
28   line by a carrier gas to the GC. The GC contains two columns and compounds are separated
29   by volatility into two fractions. The flame ionization detector (FID) monitors the
30   chromatography on two columns. After a 40 min sampling period the sample is injected into
31   the GC and the trap automatically begins collecting the next sample after 20 min ensuring
32   hourly sample acquisition.

33   Inter-comparisons with the VOC standards used by the AHN were not possible, therefore
34   uncertainties associated with the AHN standards cannot be discounted and may have

35 contributed to the offsets between the two methods. Especially in areas of high pollution,

36 datasets from automated monitoring systems using GC-FID can also be susceptible to high

37 variability, as was shown in Fortin et al., 2005, which would introduce additional uncertainty.

38 The GC-FID data were converted to ppbv using ambient pressure and temperature

39 measurements which may also have introduced some uncertainty in the AHN data.

40 **B. Calibrations and instrument background determination of the PTR-MS**

41 The multi-component VOC gas standard (Ionimed Analytik GmbH, Austria, 1ppm +/- 5%

42 uncertainty for all compounds) contained all VOCs selected for quantification by PTR-MS

43 except *m/z* 121. After the campaign it was independently validated against another multi-

44 component VOC standard (Apel Riemer Environmental Inc., CO, USA) containing the same

45 compounds with the addition of a 1,2,4-trimethylbenzene. Uncertainties for all compounds

46 were quantified in the Ionimed standard to be <10%, apart from methanol which was 15%.

47 The standard was diluted with air from the zero air generator. Normalized sensitivities were

48 between 1.4 (*m/z* 121) and 11.9 (*m/z* 45) ncps ppbv^{-1}. The original instrument used for the

49 measurements had been substantially upgraded, therefore a very similar instrument with

50 similar specifications and performance indicators was used to investigate relative changes in

51 background and sensitivity against humidity. These were thoroughly investigated in the

52 laboratory using a range of relative humidites and all variations in sensitivity were within the

53 overall calibration uncertainty (20% for methanol and <15% for all other compounds, see

54 Figure B1). Sensitivities were comparable between instruments, although those of the

55 original instrument started to decrease towards the higher masses. However, overall

56 sensitivities correlated well (r =0.94, p<0.001) and since the same instrument parameters

57 and conditions as during the campaign were maintained, it is assumed that instrument

58 responses are comparable.

59 PTR-MS sensitivities of benzene and toluene in particular have been shown to depend on

60 changes in relative humidity, i.e. when the fraction of $H_3O^+\bullet(H_2O)$ ions in the reactor change

61 (Warneke et al., 2001). For these two compounds the reaction with $H_3O^+\bullet(H_2O)$ ions is

62 energetically not permitted and does not occur (Spaněl and Smith, 2000). However, PTR-MS

63 sensitivities have a less pronounced humidity dependency at higher *E/N* ratios because the

64 reagent ions are dominated by H_3O^+ (de Gouw and Warneke, 2007). Although the absence

65 of the reaction with *m/z* 37 for these two compounds was taken into account when

66 normalising the signals, some humidity effects on background counts may have contributed

67 to the offset, as humidity effects were determined post-calibration and had to be extrapolated

68 resulting in large uncertainties.

69 A custom built zero air generator consisting of a platinum catalyst and charcoal heated to

70 200 ℃ was used to determine instrument background values. During the campaign dry air

71 was used, however this was insufficient in accounting for variations due to humidity.

72 Therefore, humidity effects were determined by humidifying the zero air over a range of

73 relative humidities in the laboratory after the campaign. The instrument background for the

74 campaign average relative humidity (72% with IQR 64-83%) was subtracted for compounds

75 showing moderate humidity dependency. For compounds with stronger humidity effects a

76 running correction based on the m/z 37/ m/z 19 ion ratio, which is a proxy for humidity, was

77 applied. These corrections produced a minimal difference due to the low variability of m/z 37

78 counts during the campaign (0.8-2.6% with a mean of 1.7% of primary ion signal). Impurities

79 in the inlet system during the campaign may have caused additional humidity dependency

80 for aromatic species. These could not be accurately recreated when investigating humidity

81 effects in the laboratory, hence this may have resulted in the remaining background offset for

82 m/z 79, 93, 107 and 121. The largest offset was seen in m/z 121, which may be due to a

83 number of factors (discussed in section 3.2 in more detail) including the fact that the

84 instrument was only calibrated against one trimethyl benzene, as standards for many of the

85 other contributing compounds were unavailable to calibrate separately. Correlations of the

86 compound against relative humidity showed low coefficients (r between 0.08 and 0.3,

87 p>0.05), which suggests most humidity effects were sufficiently accounted for, although a

88 large uncertainty associated with the quantitative measurements remains, especially for the

89 higher m/z.

90 Isobaric interferences from O_2+ ion on m/z 33 due to the $^{16}O^{17}O+$ isotope were accounted

91 for, as this reacts with the water cluster in the drift tube causing a decrease in the instrument

92 background signal with higher humidities. During the campaign, however, the O_2+ counts

93 were always <2% of the primary ion count. Additionally, interference of a CCl_4 isotope at m/z

94 121 was subtracted. Since the Montreal Protocol the addition of this compound in fire

95 extinguishers, cleaning agents, and precursors for refrigerants is prohibited and it is

96 uniformly distributed throughout the atmosphere at around 0.1 ppb. This provides a constant

97 contribution to m/z 121 in PTR-MS which can be subtracted.

98 **C. Comparison of m/z 69 with isoprene concentrations measured by GC-FID**

99 Globally isoprene is the dominant component of m/z 69, however due to the season and the

100 urban location, the biogenic contribution was absent. Comparison of the PTR-MS data for

101 m/z 69 against isoprene concentration measurements from a GC-FID at NK (courtesy of J.

102 Hopkins and R. Holmes) showed that the isoprene signal of m/z 69 was around 22% after

103 correcting for the instrument background signal (Figure C1). However, correlations with the

104 isoprene concentrations were high (r = 0.94, p<0.001). The remaining offset could be from
105 isobaric interference from other compounds such as cyclic alkanes, which share emission
106 sources with anthropogenic isoprene, in which case they represent a considerable
107 contribution to *m/z* 69 (Yuan et al., 2014). Alternatively, it may be possible that, as seen in
108 the aromatic compounds, the large uncertainties associated with the calibration (15% total
109 uncertainty) or the background corrections of the PTR-MS resulted in the offset.

References

de Gouw, J. & Warneke, C. (2007). Measurements of volatile organic compounds in the Earth's atmosphere using proton-transfer-reaction mass spectrometry. Mass Spectrometry Reviews, 26, 223– 257, doi:10.1002/mas.

Fortin, T. J., Howard, B. J., Parrish, D. D., Goldan, P.D., Kuster, W. C., Atlas, E. L. & Harley, R. A. (2005). Temporal changes in US benzene emissions inferred from atmospheric measurements, Envionrmental Science & Technology, 39(6), 1403-1408, doi:10.1021/es049316n

Oke, T. R. (2006). Towards better scientific communication in urban climate. Theoretical & Applied Climatology, 84, 179–190.

Spanĕl, P. & Smith, D. (2000). Influence of water vapour on selected ion flow tube mass spectrometric analyses of trace gases in humid air and breath. Rapid communications in mass spectrometry : RCM, 14(20), 1898–906, doi:10.1002/1097-0231(20001030)14:20<1898::AID-RCM110>3.0.CO;2-G.

Warneke, C., van der Veen, C., de Gouw, J. A., & Kok, A. (2001). Measurements of benzene and toluene in ambient air using proton-transfer-reaction mass spectrometry : calibration , humidity dependence , and field intercomparison, International Journal of Mass Spectrometry, 207, 167–182.

Yardley, R., Dernie, J., & Dumitrean, P. (2012). UK Hydrocarbon Network Annual Report for 2011, (1).

Yuan, B., Warneke, C., Shao, M. & de Gouw, J. (2014). Interpretation of volatile organic compound measurements by proton-transfer-reaction mass spectrometry over the Deepwater Horizon oil spill, International Journal of Mass Spectrometry, 358, 43-48.

133 **Table A1. Summary of site descriptions for measurements sites at North Kensington and Marylebone Rd,**
134 **London and campaign average meteorology.**

	North Kensington	Marylebone Road
Time period	16 - 25 January 2012	25 January - 7 February 2012
Site category [a]	Urban background (class A)	Urban kerbside (class A)
Area	Sion Manning School courtyard	Automatic Hydrocarbon Network[c] cabin
Coordinates (altitude)	51°31'15.18"N; 0°12'48.85"W (25m.s.l.)	51°31'21.14"N; 0°09'16.59"W (35m.s.l.)
Surroundings	Residential, <10m buildings to N and W, main road 95m E and A40 Westway 500m S (70 000- 100 000 vehicles per day)	Commercial, A501 Marylebone Rd (70 000 vehicles per day) 1.5m N, intersection Luxborough Street, Regent's Park (green area of 166 ha) 200 m N
Oke 2006 (UCZ [b]) category	3	2
Inlet height (m)	4.7	2.5
Tube length (m)	7	4
Mean temperature (°C)	7.8 ±2.9[d1]	3.0 ±2.8[d2]
Mean RH (%)	71.8 ±12.2 [d1]	68.4 ±12.0 [d2]
Precipitation (mm)	3 [d1]	11 [d2]
Mean wind speed (m s^{-1})	1 (at 4.7m) [d1]	6.4 (at 191m) [d2]
Mean wind direction (°)	205 (SSW) [d1]	62 (ENE) [d2]

135 [a]Site classification: Category A indicates sites highly representative of emissions for intended areas.
136 [b] Urban Climate Zone classifications by Oke, 2006.
137 [c] Permanent measurement site run by the Department for Environment, Food and Rural Affairs (DEFRA)
138 [d1] Data from WXT520 weather sensor (Vaisala Ltd, Finland) at NK
139 [d2] Data from WXT520 weather sensor at BT tower near MRd

140

141 **Figure captions**

142 **Figure A1. Top)** Representation of the PTR-MS measurement cycle used at both North
143 Kensington and Marylebone Rd sites. The multiple ion detection (MID) cycle lasted 20.5 sec
144 and was repeated during 25 min. **Bottom)** Approximation of the measurement cycle used by
145 the Automatic Hydrocarbon Network GC-FID at the Marylebone Rd measurement site.
146 Multiple sample analyses are indicated by *a* (previous hour), *b* (hour 1.) and *c* (hour 2.).
147 Each cycle consists of the following stages: 1. Sample acquisition (40 min), 2. analytes are
148 injected into GC columns, 3. trap cooling in preparation for the next sample acquisition (15
149 min), 4. GC analysis (50 min), and 5. GC cooling in preparation for the next sample analysis
150 (Yardley et al., 2012).

151 **Figure B1.** Post-campaign calibrations over a range of relative humidities (0, 30, 60, 90% +/-
152 5%) for all nine selected compounds (methanol [*m/z* 33], acetonitrile [*m/z* 42], acetaldehyde
153 [*m/z* 45], acetone [*m/z* 59], isoprene [*m/z* 69], benzene [*m/z* 79], toluene [*m/z* 93], o-xylene
154 [*m/z* 107], and 1,2,4-trimethylbenzene [*m/z* 121]) .

155 **Figure C1.** Comparison of 1 h averages of *m/z* 69 (ppb) measured by PTR-MS against
156 isoprene concentrations measured by GC-FID (ppb) at North Kensington during 16th – 25th
157 Jan 2012 showing the linear regression with correlation coefficient (r). We gratefully
158 acknowledge James Hopkins and Rachel Holmes (University of York) for making the data
159 available for analysis.

160